

AD_____

Award Number: W81XWH-11-1-0284

TITLE: A tailored approach to prostate cancer therapy based upon PTEN status.

PRINCIPAL INVESTIGATOR: Phyllis Wachsberger, Ph.D.

CONTRACTING ORGANIZATION: Jefferson Medical College
Philadelphia, PA 19107

REPORT DATE: November 2012

TYPE OF REPORT: Final

PREPARED FOR: U.S. Army Medical Research and Materiel Command
Fort Detrick, Maryland 21702-5012

DISTRIBUTION STATEMENT: Approved for Public Release;
Distribution Unlimited

The views, opinions and/or findings contained in this report are those of the author(s) and should not be construed as an official Department of the Army position, policy or decision unless so designated by other documentation.

Table of Contents

	<u>Page</u>
Cover Page.....	1
Table of Contents.....	2
Report Documentation Page.....	3-4
Introduction.....	4
Body.....	5-7
Key Research Accomplishments.....	8
Reportable Outcomes.....	8
Conclusion.....	8
References.....	8
Appendices.....	9-37

REPORT DOCUMENTATION PAGE				Form Approved OMB No. 0704-0188	
Public reporting burden for this collection of information is estimated to average 1 hour per response, including the time for reviewing instructions, searching existing data sources, gathering and maintaining the data needed, and completing and reviewing this collection of information. Send comments regarding this burden estimate or any other aspect of this collection of information, including suggestions for reducing this burden to Department of Defense, Washington Headquarters Services, Directorate for Information Operations and Reports (0704-0188), 1215 Jefferson Davis Highway, Suite 1204, Arlington, VA 22202-4302. Respondents should be aware that notwithstanding any other provision of law, no person shall be subject to any penalty for failing to comply with a collection of information if it does not display a currently valid OMB control number. PLEASE DO NOT RETURN YOUR FORM TO THE ABOVE ADDRESS.					
1. REPORT DATE November 2012		2. REPORT TYPE Final		3. DATES COVERED 15 April 2011- 14 October 2012	
4. TITLE AND SUBTITLE "A Tailored Approach to Prostate Cancer Therapy Based upon PTEN Status"				5a. CONTRACT NUMBER	
				5b. GRANT NUMBER W81XWH-11-1-0284	
				5c. PROGRAM ELEMENT NUMBER	
6. AUTHOR(S) Phyllis Wachsberger, Ph.D E-Mail: Phyllis.wachsberger@jeffersonhospital.org				5d. PROJECT NUMBER	
				5e. TASK NUMBER	
				5f. WORK UNIT NUMBER	
7. PERFORMING ORGANIZATION NAME(S) AND ADDRESS(ES) Jefferson Medical Center Philadelphia PA 19107				8. PERFORMING ORGANIZATION REPORT NUMBER	
9. SPONSORING / MONITORING AGENCY NAME(S) AND ADDRESS(ES) U.S. Army Medical Research and Materiel Command Fort Detrick, Maryland 21702-5012				10. SPONSOR/MONITOR'S ACRONYM(S)	
				11. SPONSOR/MONITOR'S REPORT NUMBER(S)	
12. DISTRIBUTION / AVAILABILITY STATEMENT Approved for Public Release; Distribution Unlimited					
13. SUPPLEMENTARY NOTES					
14. ABSTRACT- The purpose of this study was to investigate the hypothesis that PTEN null prostate cancer cells and tumors will exhibit increased radiosensitivity to inhibition of the DNA repair enzyme, PARP, compared to wild-type PTEN-expressing cells and tumors, resulting in increased efficacy of radiotherapy and chemotherapy. The specific objectives of this study were to (1) determine the effect of PARP inhibition on the cellular response to ionizing radiation or docetaxel in DU145 PTEN wild-type vs. PC-3 PTEN-null cells. and (2): determine the efficacy of PARP inhibition in combination with radiotherapy or docetaxel in DU145 and PC-3 prostate cancer xenograft models. Radiosensitization was measured in DU145 cells and PC-3 cells by <input type="checkbox"/> H2AX foci formation and disappearance, quantitation of olive tail moment in comet assay, clonogenic cell survival and apoptosis assay. Additionally, qPCR was performed to assess changes in DNA repair gene expression following radiation and/or drug treatments. <input type="checkbox"/> H2AX foci assays revealed that ABT888 in combination with radiation therapy (RT) increased the level of DNA damage compared to drug alone and RTX alone in both cell lines, and that the combination inhibited DNA repair in PC-3 cells but not in DU145 cells. Apoptosis assays indicated that DU145 cells were more susceptible than PC-3 cells to apoptosis induction by monotherapy with ABT888, docetaxel or RT. However, triple modality treatment with ABT888, docetaxel and RT increased apoptosis similarly in both cell lines. Clonogenic assays revealed that although DU145 was more radioresistant than PC-3 cells, ABT888 similarly radiosensitized both cell lines. qPCR revealed prolonged upregulation of the RAD family members in PC-3 cells. In vivo studies of tumor growth confirmed that the PC-3 xenografts, lacking PTEN, were more sensitive to RT than the DU145 xenografts. However, ABT888 did not increase radiosensitivity significantly in either xenograft. Ongoing work on isogenic models of PTEN wt and PTEN prostate cancer models will help to clarify the role of PTEN in radiosensitizing tumors to PARP inhibitors.					
15. SUBJECT TERMS- PC-3, DU145, PTEN, radiosensitization, ABT888, Docetaxel					
16. SECURITY CLASSIFICATION OF:			17. LIMITATION OF ABSTRACT	18. NUMBER OF PAGES	19a. NAME OF RESPONSIBLE PERSON
a. REPORT U	b. ABSTRACT U	c. THIS PAGE U			USAMRMC
			UU	37	19b. TELEPHONE NUMBER (include area code)

Introduction

This proposal specifically focuses on the PTEN tumor suppressor and its interaction with the poly (adenosine diphosphate [ADP]–ribose) polymerase (PARP) DNA repair pathway in advanced prostate cancer (APC). It examines the hypothesis that PTEN deficiency induces chemo/radioresistance in APC that can be specifically overcome through PARP inhibition. This hypothesis was based on the observation that PTEN affects double-strand breaks through regulation of Rad51, a key player in homologous recombination repair (HRR) of DNA double strand breaks (DSBs).¹ It was speculated that PTEN null cells have DNA repair deficiencies in the HRR pathway that will compromise their ability to repair DNA DSBs and will therefore be highly sensitive to PARP inhibition of DNA repair. Several measures of DNA damage and repair were proposed to assess radiosensitization in vitro in PTEN wild-type (DU145) vs. PTEN-null (PC-3) cells. In vivo studies were proposed to determine the efficacy of PARP inhibition in combination with radiotherapy or docetaxel in PTEN wild-type and PTEN-null human prostate cancer xenograft models implanted in nude mice.

Body

Task 1: Determine how PTEN status impacts the response to DNA damage following chemo/radiation in the absence or presence of PARP inhibition

1a. γ H2AX assay. The number of DNA double strand breaks (DSBs) was assessed by quantification of γ H2AX foci based on a previously published protocol². Briefly, fixed cells were analyzed for γ H2AX 30 min and 24 hrs following treatments. Primary anti-phospho- γ H2AX mouse monoclonal antibody was added at a dilution of 1:300 in 5% bovine serum albumin (BSA). Secondary Alexa Fluor 594 donkey anti-mouse antibody (Invitrogen Molecular Probes, Eugene OR) was added at a dilution of 1:500 in 5% BSA. Cells were counterstained with DAPI incorporated into ProLong Gold mounting medium (Invitrogen, Molecular Probes, Eugene OR) for nuclei visualization. γ H2AX foci visualization was performed on a Zeiss LSM 510 Meta Confocal Microscope (Carl Zeiss Microscope Inc., Thornwood, NY) using a 40X oil immersion lens and analyzed by Image J software provided by NIH.

Assays were performed 30 min and 24 hrs following radiation in order to measure maximum and residual damage (i.e., following DNA repair)

Results:

Figure 1 indicates that ABT888 alone induced more immediate DNA damage, although not significantly, in PC-3 vs. DU145 cells ($p = 0.09$), and inhibited DNA repair in PC-3 cells vs. DU145 cells ($P = 0.001$). Radiation (RT) alone inhibited repair in PC-3 cells ($p = 0.01$). The combination of ABT888 + RT inhibited DNA repair in PC-3 cells but not in DU145 cells ($p = 0.04$).

Effect of Docetaxel on gamma H2AX assay: Docetaxel at a concentration of 5 nM induced apoptosis in both PC-3 and DU145 cells which made it difficult to assess for γ H2AX foci induction in the largely apoptotic nuclei. Therefore experiments with docetaxel were not analyzed for γ H2AX foci.

1b. Comet assay. The kinetics of DNA DSBs and repair was assessed by measuring olive tail moment using Trevigen's CometAssay kit under alkaline conditions (Gaithersburg, MD). Comet Score image analysis software was used to calculate olive tail moment which is a relative measure of DNA damage.

Results:

Figure 2 - 4 show the response of DU145 and PC-3 cells to radiation doses (0 – 30 Gy). A dose dependent response is evident. Based on these observations, a dose of 15 Gy was selected to test the effect of ABT888 on the kinetics of DNA repair following radiation.

Figures 5-10 indicate that ABT888 + RT enhances initial DNA damage and slows down DNA repair following 15 Gy RT in both cell lines. The kinetics of repair up to 30 min was not significantly different between cell lines.

This data, is confirmatory with the γ H2AX assay data, since both assays indicate that DNA repair is compromised 30 min following ABT888 and radiation. However, the γ H2AX foci assay, which was assessed 24 hr following treatment, distinguishes between PC-3 and DU145 cells in that it demonstrated prolonged DNA repair inhibition in PC-3 cells compared to DU145 cells.

Figures 11-16 show the effect of triple modality treatment, i.e., docetaxel + ABT888 + RT on DNA damage and repair kinetics in DU145 vs. PC-3 cells. No significant differences were seen between cell lines..

1c. Cell Survival Assay. Clonogenic cell survival assay was performed as previously described³, with exponentially growing cells with and without ABT888 treatment for 24 hr. Data was fit to a linear quadratic model for cell survival. The mean \pm SEM from at least three independent experiments were obtained.

Results:

Figure 17 shows ABT888 at 100 μ M reduces clonogenicity in both cell lines to approximately 60%. Therefore ABT888 at 100 μ M was chosen to study its radiosensitizing potential.

Figure 18 indicates that DU145 cells are more radioresistant than PC-3 cells, as determined by a smaller alpha (α) value (0.028) (initial slope of curve) than seen in PC-3 cells ($\alpha = 0.09$). ABT888 acts as a radiosensitizer in both DU145 and PC-3 cells as determined by an increase in α of the survival curves from 0.028 to 0.14 and

from 0.09 to 0.36 in DU145 and PC-3 respectively. The sensitizer enhancement ratios calculated as the ratio of the initial slopes (α) of survival curves were not significantly different (5 ± 2 and 4 ± 3.0 for DU145 and PC-3 respectively, $p = 0.9$) from each other. Therefore, the relative degree of radiosensitization was similar in both cell lines after ABT888 treatment.

1d qPCR assays

Alterations in DNA Repair gene expression in PC-3 (PTEN Null) and DU145 (PTEN wt) prostate cancer cells following 24 treatment with ABT888 and/or radiation

Raw data from the RT PCR reactions were analyzed using RT² Profiler PCR Array Data Analysis from SABiosciences (<http://www.sabiosciences.com/pcrarraydataanalysis.php>). B2M, HPRT1, ACTB, GAPDH and RPLP0 were the house keeping genes selected for the baseline. $\Delta\Delta C_t$ based fold-change calculations were performed and transformed using log base 2. The data were inspected for genomic contamination prior to analysis. Genes were selected based on the magnitude of log 2 transformed fold change of ≥ 2 compared to control and were considered to play a direct role in the homologous recombination repair pathway (HRR) in which PTEN plays a role. All experiments were performed in triplicate at time point of 24 hr following treatment.

For PC-3 cells, a total of 6 genes out of 87 DNA repair genes were selected for further analysis. These genes were up-regulated in response to any treatment combination and included most of the RAD protein family members. (**Fig. 19**). Sole treatment with PARP inhibitor, ABT888, resulted in a fold change of 2 in RAD 51 B which did not reach significance ($P=0.1$). RT alone significantly increased RAD51, RAD54L and RPA3 >2-fold ($p < 0.04$). ABT888 + RT increased RAD50 significantly ($p = 0.005$) and RAD51B and RPA3 >2-fold, however, not significantly ($p = 0.2$ and 0.1 respectively). The prevalence of upregulated RAD family genes in PC-3 cells 24 hr following treatments most likely reflects the inability of PC-3 cells lacking PTEN to efficiently repair DSB damage through the HRR pathway, and therefore results in prolonged upregulation of these repair genes at 24 hr. In contrast to PC-3 cells, the RAD repair genes in the DU145 cell line were down-regulated or close to control levels under all treatment conditions (**Fig.20**), with no fold changes reaching significance. DU145 possesses a functional PTEN allowing for efficient HR repair of DSB breaks, even in the presence of PARP inhibition; consequently after 24 hrs, DU145 cells likely completed repair of the DNA lesions and are consequently downregulating repair genes or returning them to control levels.

1f. Apoptosis Assay. Cells were treated with ABT888 (50 μ M) and Docetaxel (5 nM) for 24 hr. Radiation was administered at 6 Gy following drug treatments. Cells were collected 24 hr post radiation for apoptosis evaluation using an FITC Annexin V and propidium iodide kit (BD Pharmingen) and analyzed by flow cytometry (Coulter (XL-MCL). Tabulation of percentage of cells undergoing early and late apoptosis (Figure 22) is based on graph shown in Figure 11.

Results:

Figures 21 and 22 indicate DU145 cells are more susceptible than PC-3 cells to apoptosis after treatment with RT alone, docetaxel alone and ABT888 alone. DU145 cells are also more susceptible than PC-3 cells to apoptosis after treatment with ABT888 + docetaxel and docetaxel + RT. Since PTEN suppresses signaling in the anti-apoptotic PI3K/Akt pathway, the presence of PTEN wildtype in this cell line may explain the tendency to undergo apoptosis more readily than the PTEN null PC-3 cell line. However, both cell lines are equally susceptible to apoptosis following treatment with ABT888 + RT. Furthermore, triple modality treatment with ABT888, docetaxel and RT increases apoptosis in both cell lines.

Task 2. Determine the efficacy of PARP inhibition in combination with radiotherapy or docetaxel in vivo in two human prostate cancer xenograft models

2a. Establish prostate tumor xenografts in nude mice.

PC-3 and DU145 tumor cell suspensions (1×10^7 cells in 100 μ l phosphate buffered saline) from each tumor cell line were implanted subcutaneously into the right hind limbs of athymic NCR NUM mice (Taconic Farms, Hudson, NY). Mice were not pretreated before tumor implantation. Tumors were allowed to grow for approximately 3-4 weeks until reaching an approximate volume of 80-200 mm³ before start of treatment (day 0) and were measured 3-4 times per week, for up to 60 days of follow-up, or until they reached 2,000 mm³ (in

accordance with IACUC regulations). Tumors were randomized into treatment groups when they reached appropriate size.

Results;

Tolerability studies in non-tumored animals

Figure 23 shows tolerability data for the drugs, ABT888 and Docetaxel. The results indicate that at the doses given (ABT888 at 100 mg/kg daily and Docetaxel, 15 mg/kg, Day 0 and Day 7), there is no toxicity with regard to body weight as an endpoint. Therefore these doses were used in tumored animal studies.

2b. Tumor Growth Delay:

DU145 xenografts

The experiment involved treatments with docetaxel (administered once daily on Day 0 and Day 7), ABT-888 (administered daily for two weeks on days 0-4 and days 7-11), and radiation (RTX) given as three daily fractions of 3 Gy on days 0, 1 and 2. Mixed effects linear regression was used to model log₁₀-transformed tumor volumes. Fixed effects were time, treatment group, and group by time interaction. Random effects included the intercept and time. Together, this model fits a linear curve in time to each animal and averages across animals in each group to obtain a group-average linear curve in time for the log-10 transformed tumor volumes. This model allows for the estimation of geometric mean tumor volumes at any time as well as the rate of change (expressed as a geometric mean ratio or percentage change per day) in tumor volume at any time. All analyses were performed using SAS 9.3 (SAS Institute, Cary, NC).

For these analyses, animals determined to be necrotic or sick were excluded.

Results:

The analyses were based on a total of 2223 tumor size measurements from 70 animals (up to 8.5 weeks of follow-up (Table 1)).

Linear tumor growth curves fit the data well, with tumors continuing to grow throughout the observation period of 0 to 60 days in most animals. The results of the tumor growth for the 8 experimental groups are summarized in Table 2 and displayed in Figure 24.

Table 3 gives the growth rates expressed as the percentage change in volume per day for each group along with the tumor doubling time for each group. P-values for selected pairwise comparisons of growth rates are given in Table 4. The control group grew fastest. Growth in the radiation only group and drug only groups was slower but not significantly different from that of the control group. The ABT-888 and RTX group grew slower than the RTX group but did not reach significance. Thus, ABT888 did appear to improve radiotherapy in the DU145 xenografts; however, because of low animal numbers per group due to loss of animals in the early stages of the study, the degree of variability was high and therefore differences in growth rates did not reach significance. This study would need to be repeated with larger animal numbers to make the conclusion about ABT888's effect on radiosensitivity conclusive.

PC-3 xenografts

The analyses were based on a total of 2233 tumor size measurements from 86 animals (up to 8.5 weeks of follow-up (Table 5)).

Linear tumor growth curves fit the data well, with tumors continuing to grow throughout the observation period of 0 to 60 days in most. The results of the tumor growth for the 8 experimental groups are summarized in Table 6 and displayed in Figure 25.

Table 7 gives the growth rates expressed as the percentage change in volume per day for each group along with the tumor doubling time for each group. P-values for selected pairwise comparisons of growth rates are given in Table 8. The control group grew fastest. When compared with DU145 controls, PC-3 tumors grew faster (tumor doubling time = 9.2 days vs. 13.9 days respectively ($p < 0.05$)). (The rate of growth was significantly reduced by RTX and Docetaxel, but not by ABT-888 alone. RTX + ABT-888 led to slower tumor doubling times than ABT-888 alone ($p = 0.009$), and RTX alone (although this comparison did not reach significance ($P = 0.32$)). In addition, the combination of ABT-888 and Docetaxel was nearly significantly worse (faster) than Docetaxel alone ($p = 0.075$)).

Key Research Accomplishment

- **ABT888 has been shown to be an effective radiosensitizer in prostate cancer cell lines in vitro, DU145 and PC-3, through a number of DNA damage assays, which were all confirmatory.**
- **In vivo, ABT888 + RTX was better than RTX in both DU145 or PC-3 xenografts.**
- **qPCR data indicate prolonged expression of homologous recombination repair enzymes in PC-3 compared to DU145 cells**

Reportable Outcomes

None to date

Conclusion

The PARP inhibitor, ABT888, potentiates radiation-induced damage in DU145 (PTEN wildtype (wt)) and PC-3 cells (PTEN null) cells. DNA repair was more compromised in PTEN null cells than in DU145 cells, based on γ H2AX assays. qPCR analyses indicated prolonged expression of repair genes in PC-3 cells compared to DU145 cells, and therefore the extent to which DNA repair systems were perturbed by ABT888 and radiation. Additional qPCR analyses may help in the development of DNA repair biomarkers which may be used to stratify patient population likely to benefit from PARP inhibitor therapies. With regard to PTEN status, data from the apoptosis and clonogenic survival assays seem to indicate radiosensitization is independent of PTEN status in these cells. In vivo data confirmed that the PC-3 xenografts, lacking PTEN, and the DU145 xenografts are both radiosensitized by ABT888. However, because of high variability within treatment groups, relative radiosensitization by ABT888 in PC-3 vs. DU145 xenografts needs to be determined by additional studies with higher numbers of animals. Further work on isogenic models of PTEN wt and PTEN prostate cancer models are ongoing to help clarify the role of PTEN in radiosensitizing tumors to PARP inhibitors.

References

1. Shen WH, Balajee AS, Wang J, Wu H, Eng C, Pandolfi PP, Yin Y. Essential role for nuclear PTEN in maintaining chromosomal integrity. *Cell*, 2007 January 12;128(1):157-70.
2. Munshi A, Tanaka T, Hobbs ML, Tucker SL, Richon VM, Meyn RE. Vorinostat, a histone deacetylase inhibitor, enhances the response of human tumor cells to ionizing radiation through prolongation of gamma-H2AX foci. *Mol.Cancer Ther.* 2006;5:1967-74.
3. Wachsberger PR, Lawrence RY, Liu Y, Xia X, Andersen B, Dicker AP. Cediranib enhances control of wild type EGFR and EGFRvIII-expressing gliomas through potentiating temozolomide, but not through radiosensitization: implications for the clinic, *J Neurooncol.* 2011 105 (2): 181-90.

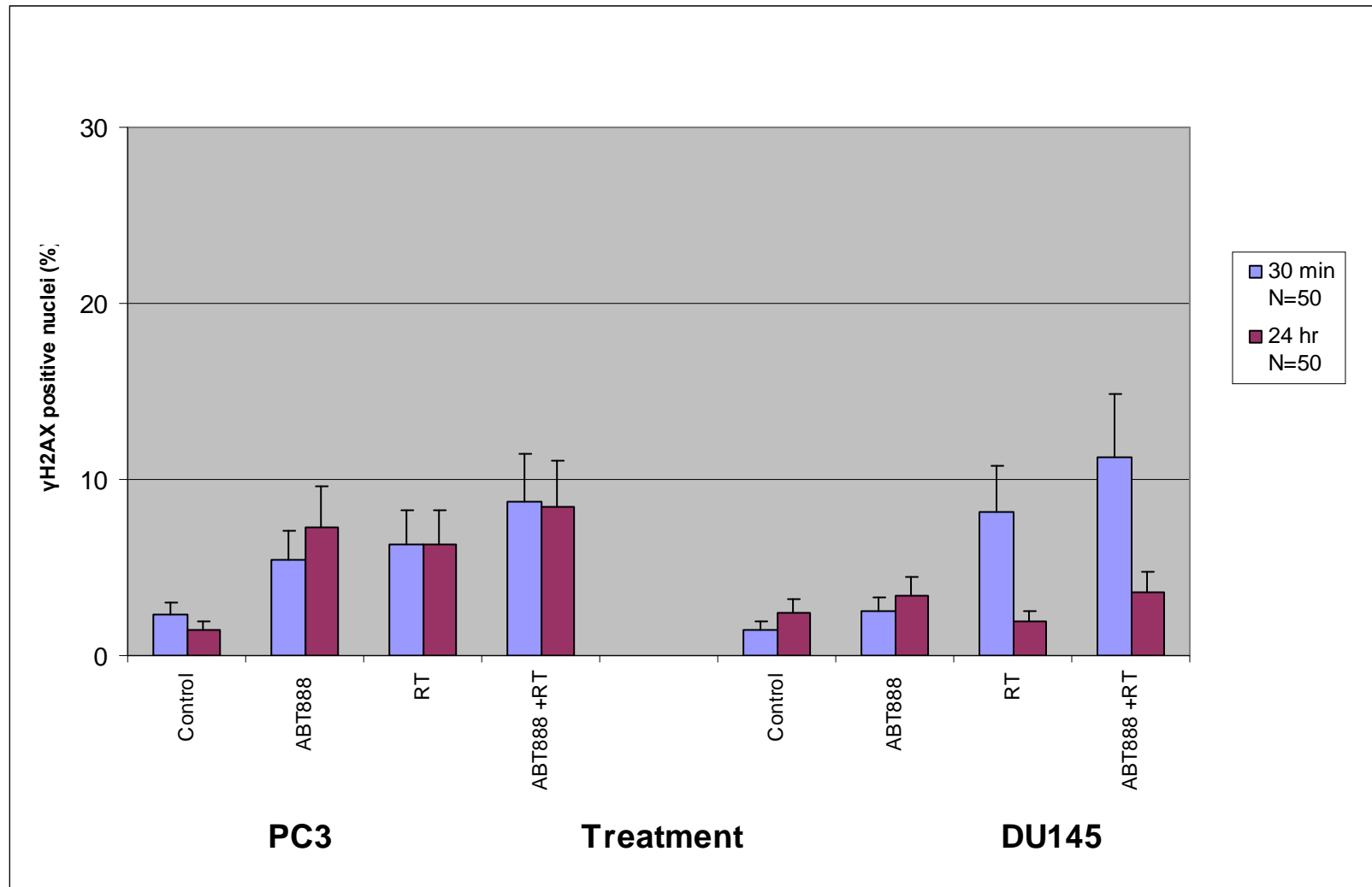
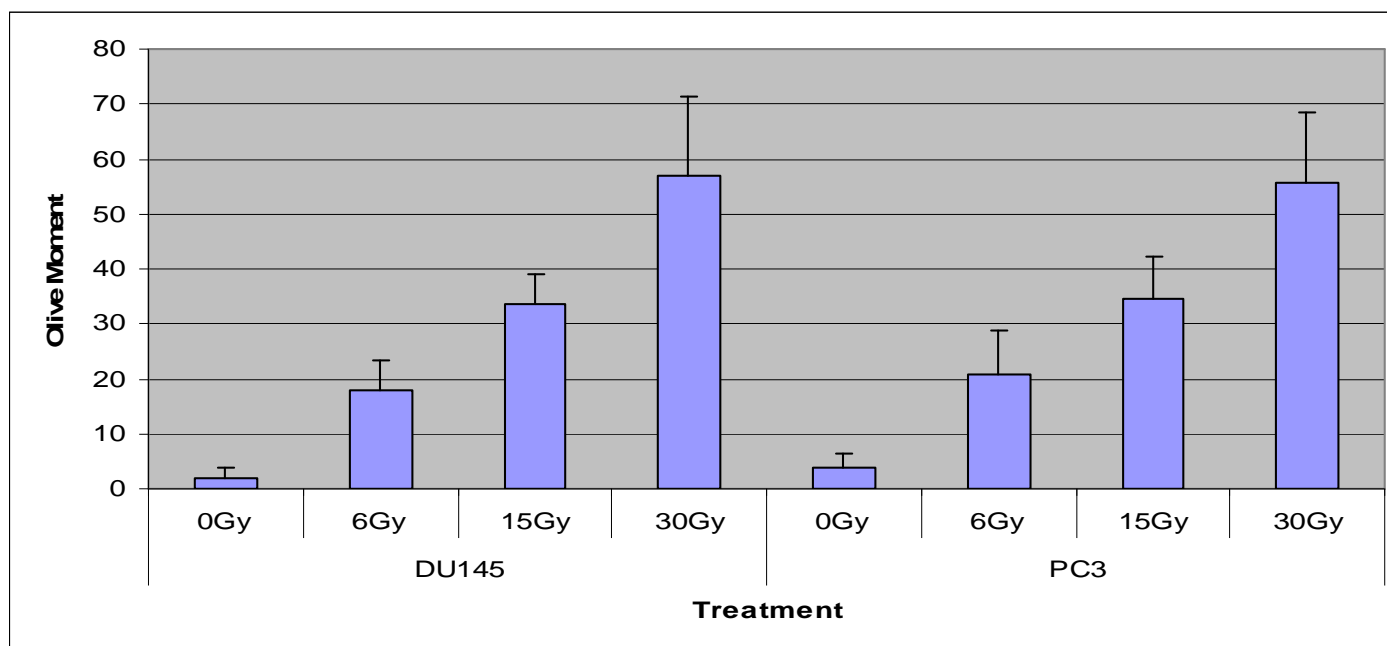


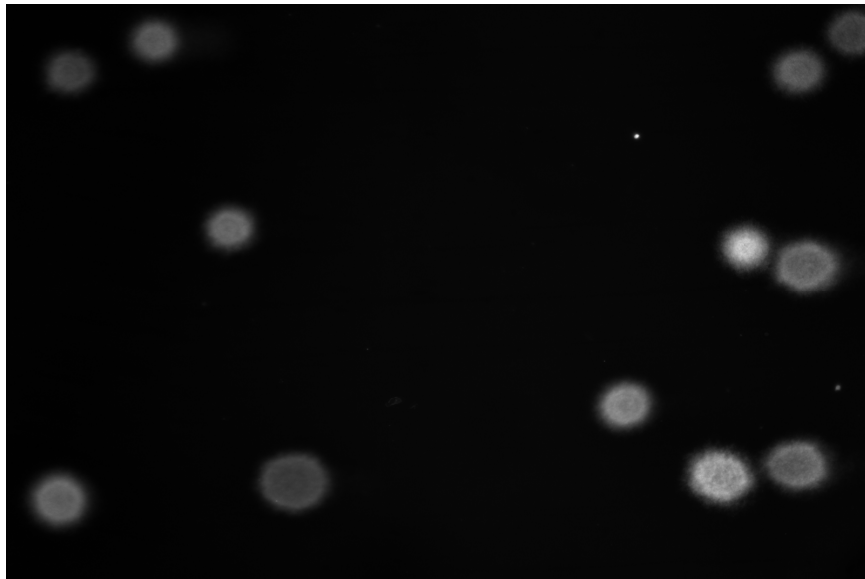
Figure 1. Effect of ABT888 (50 μ M) and/or RT on induction of γ H2AX foci in PC3 and DU145 cells. Cells containing nuclei with 3 or more γ H2AX foci were classified as positive for DNA damage. 50 nuclei were counted for each treatment 30 min and 24 hr post RT (2 Gy). The mean \pm SEM from at least three independent experiments were obtained with three replicates per experiment.



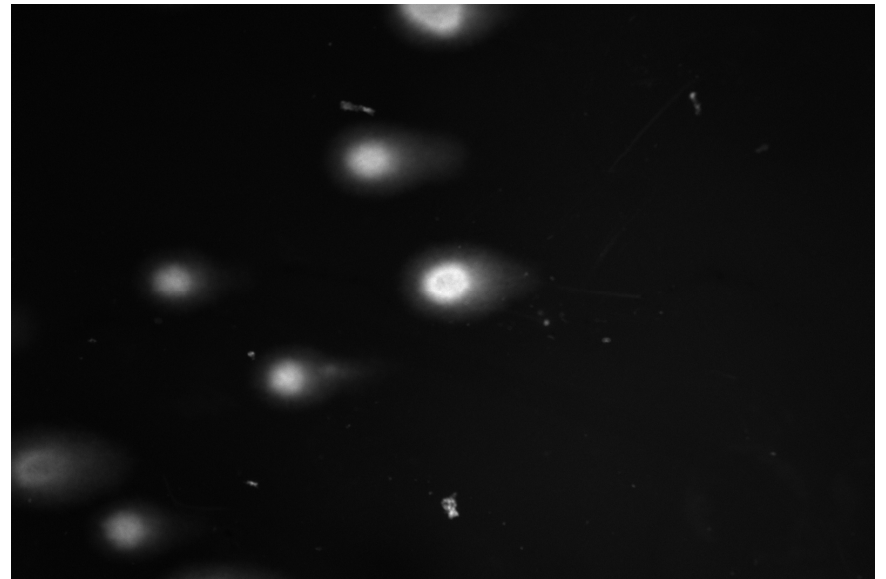
		N	Mean	Stdev
DU145	0Gy	48	2.01	1.85
	6Gy	42	17.82	5.45
	15Gy	54	33.61	5.49
	30Gy	40	56.91	14.35
PC3	0Gy	32	3.88	2.44
	6Gy	28	20.65	8.06
	15Gy	40	34.42	7.73
	30Gy	42	55.83	12.64

Figure 2. Comet Assay. Effect of radiation dose escalation on olive moment in DU145 and PC-3 cells. Cells were prepared for Comet assay according to instructions given in Trevigen kit.

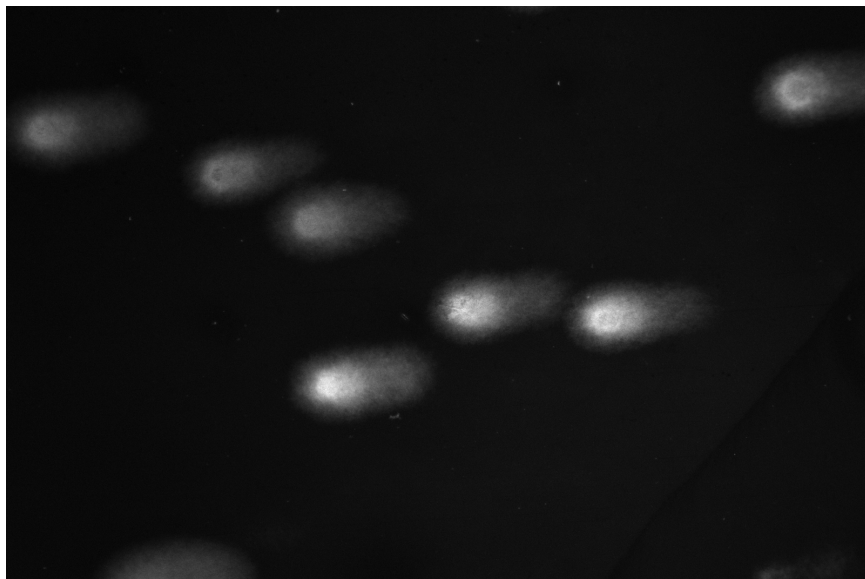
DU145, 0Gy



DU145, 6Gy



DU145, 15Gy



DU145, 30Gy

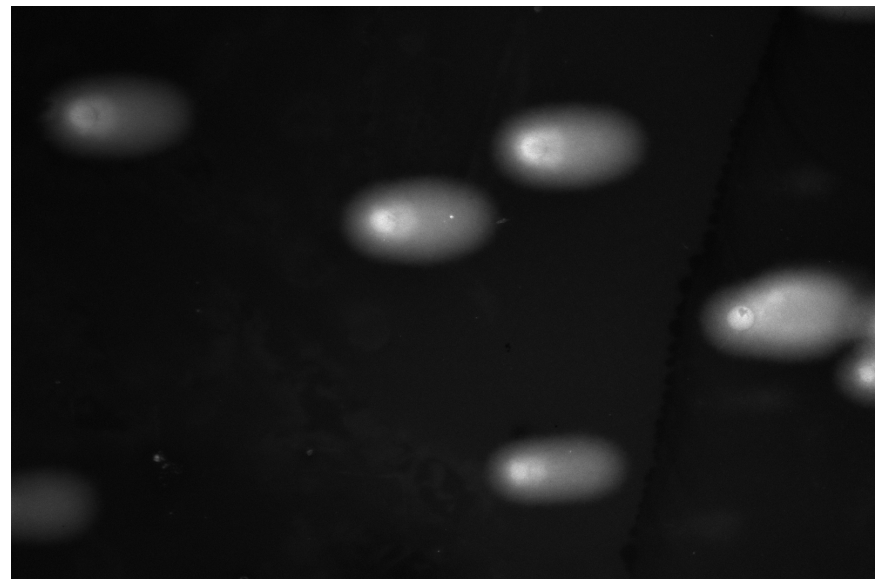
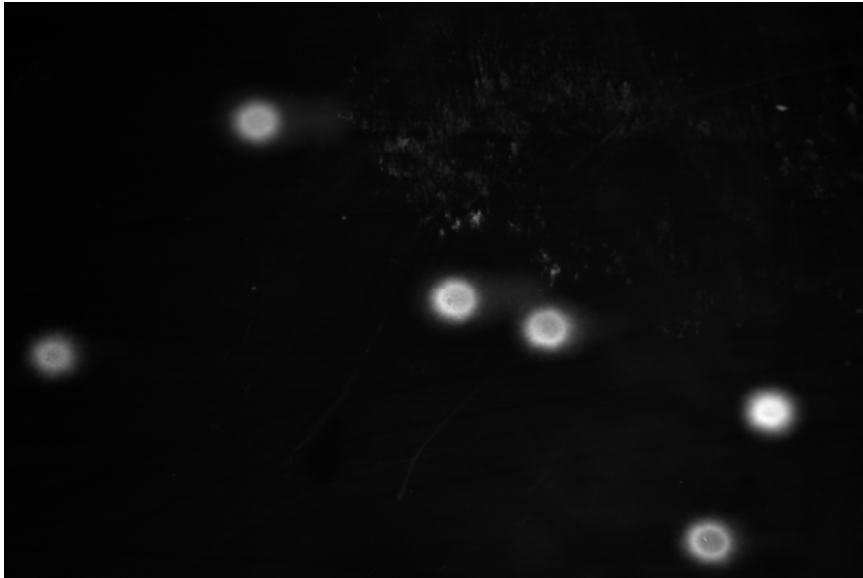
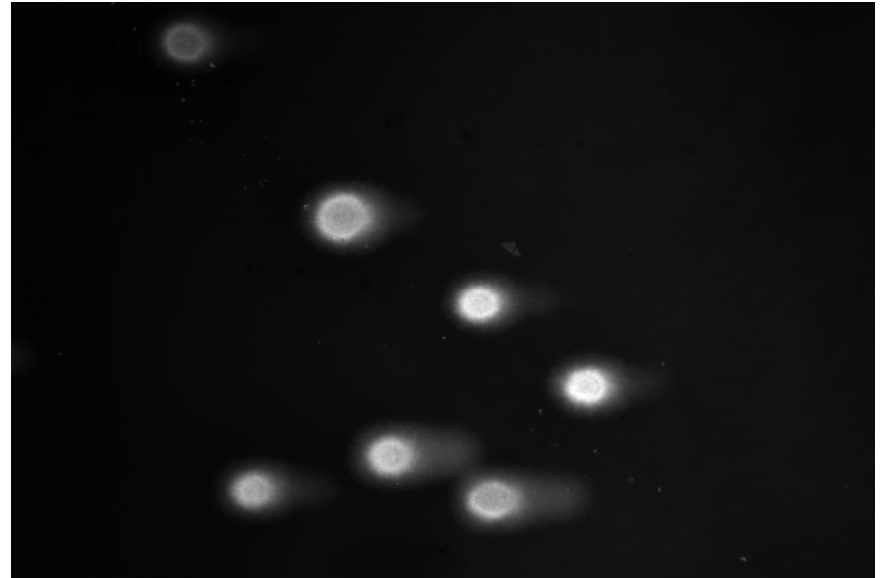


Figure 3. Comet images showing comet tails increasing with increasing dose of RT in DU145 cells.

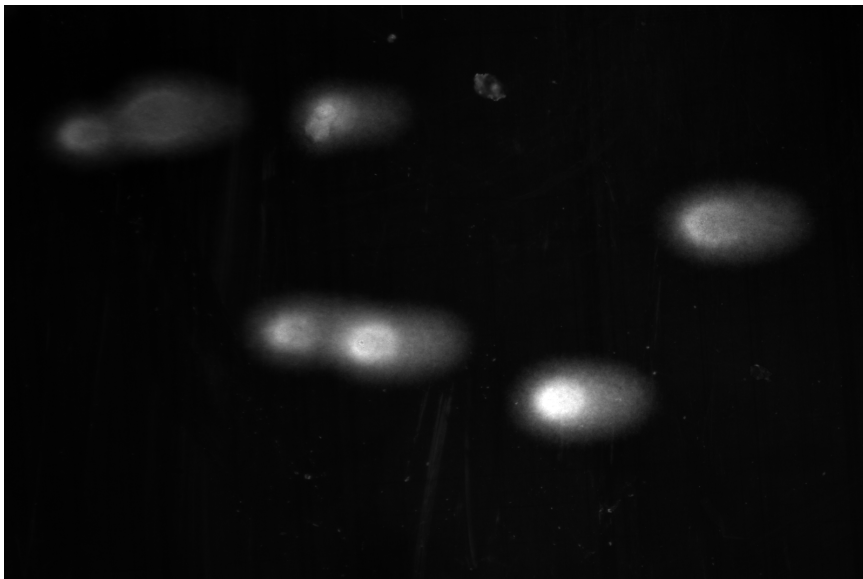
PC3, 0Gy



PC3, 6Gy



PC3, 15Gy



PC3, 30Gy

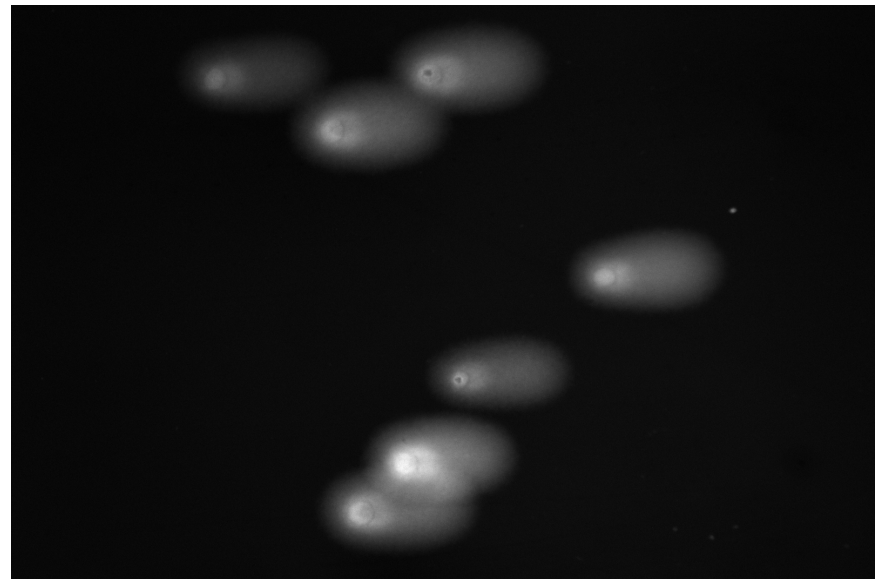
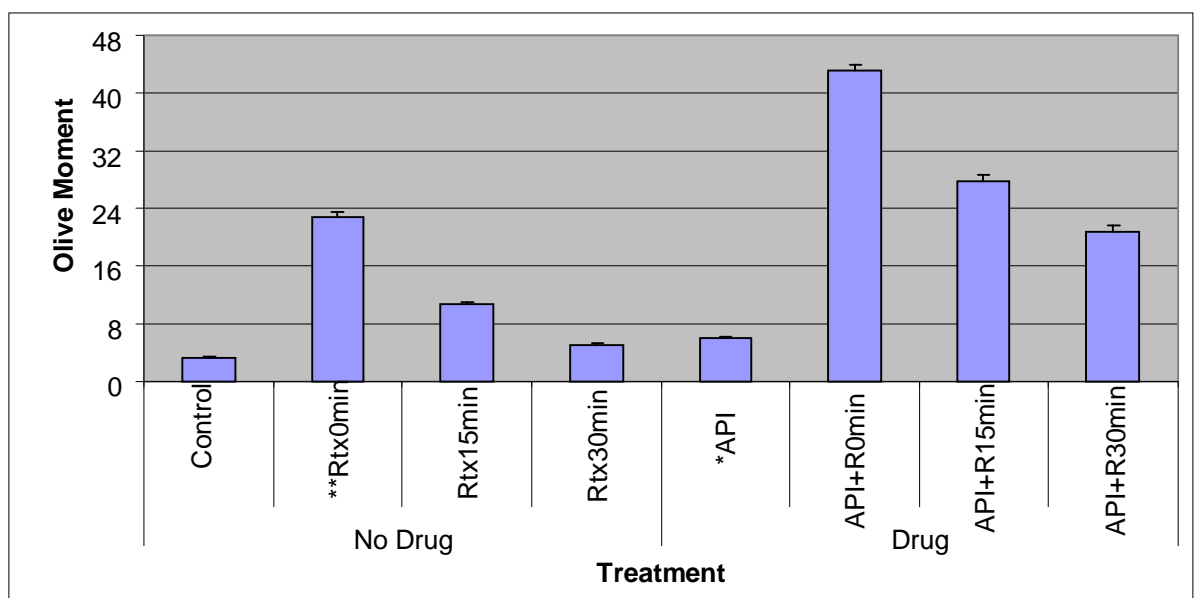


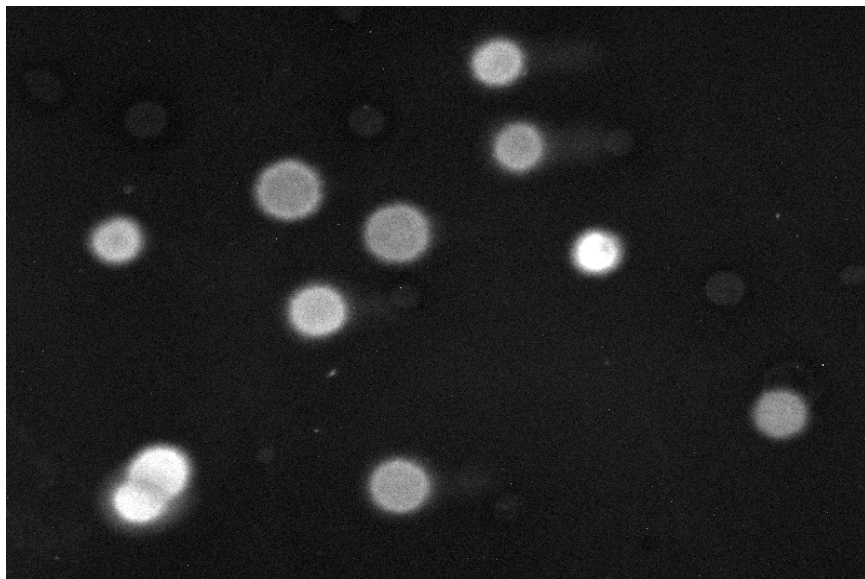
Figure 4. Comet images showing comet tails increasing with increasing dose of RT in PC-3 cells.



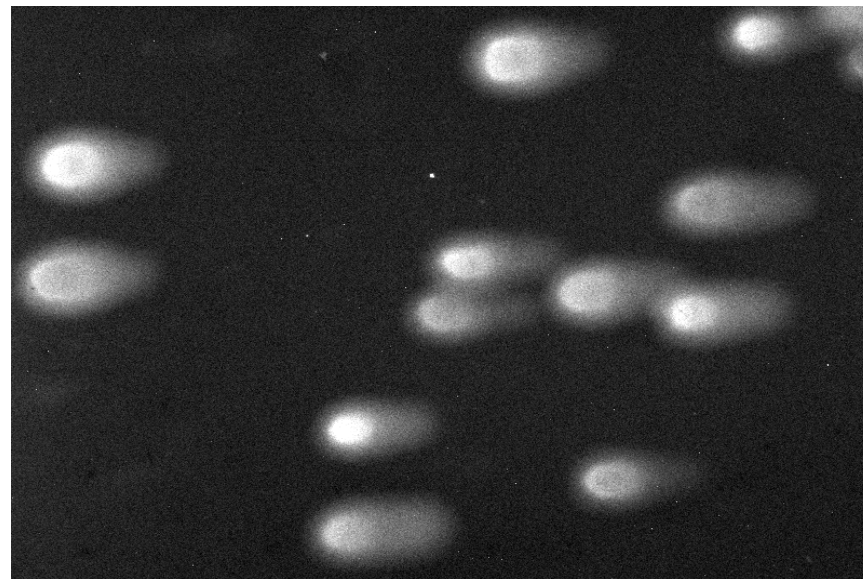
		N	Mean	Stdev	Stderr
No Drug	Control	56	3.27	1.43	0.191092
	Rtx0min	52	22.78	4.78	0.662867
	Rtx15min	59	10.73	2.29	0.298133
	Rtx30min	53	5.01	2.34	0.321424
Drug	API	65	6.04	1.66	0.205898
	API+R0min	36	43.11	4.69	0.781667
	API+R15min	42	27.84	5.42	0.836324
	API+R30min	48	20.80	4.99	0.720244

Figure 5. Comet Assay. Quantification of olive moment as a measure of kinetics of DNA repair in DU145 cells. *API = Abbott PARP Inhibitor (ABT888) (50µM); **Rtx = radiation (15 Gy)

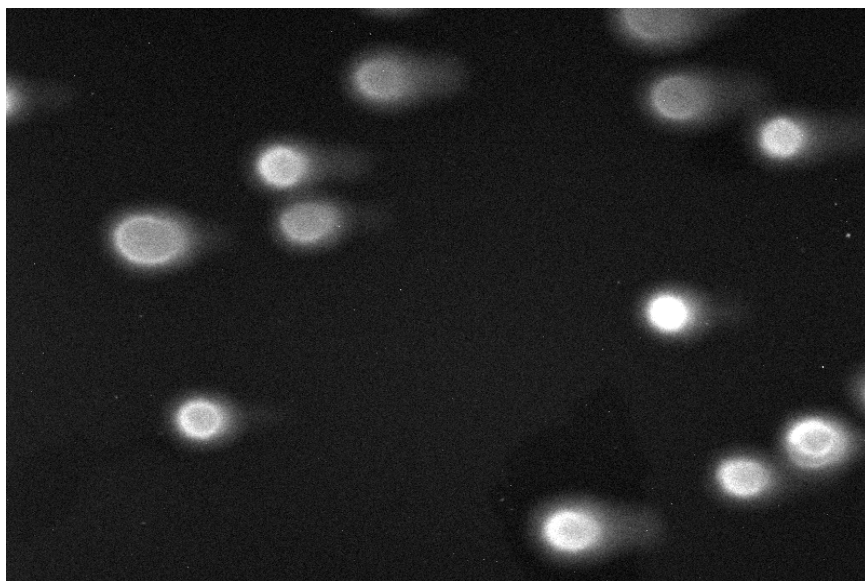
Control



Rtx, 0min



Rtx, 15min



Rtx, 30min

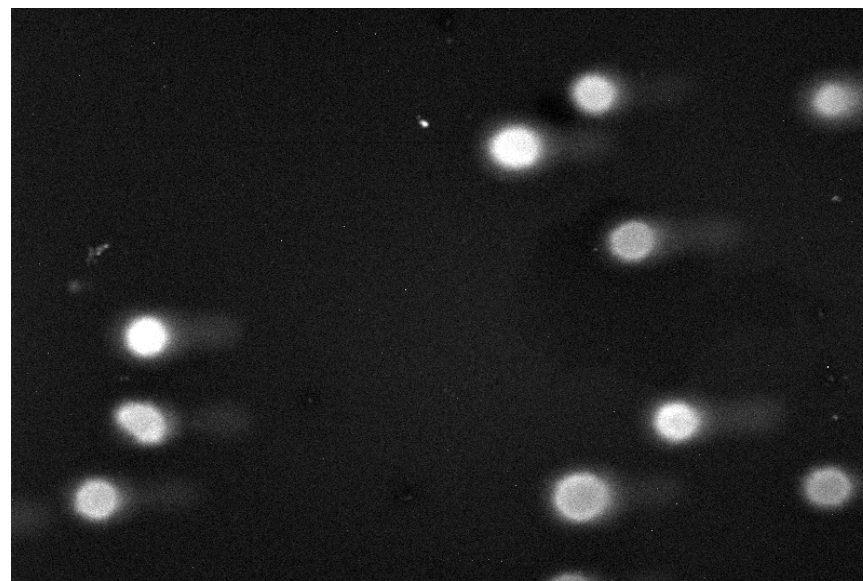
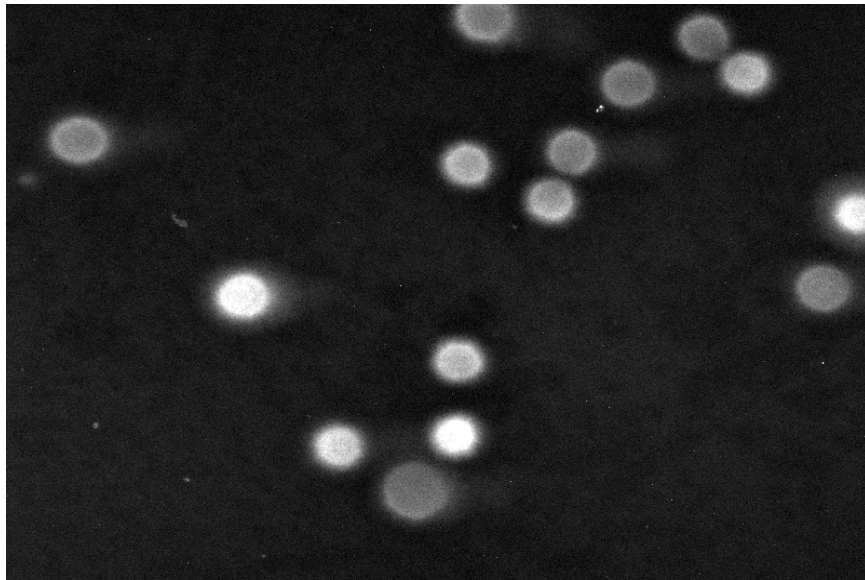
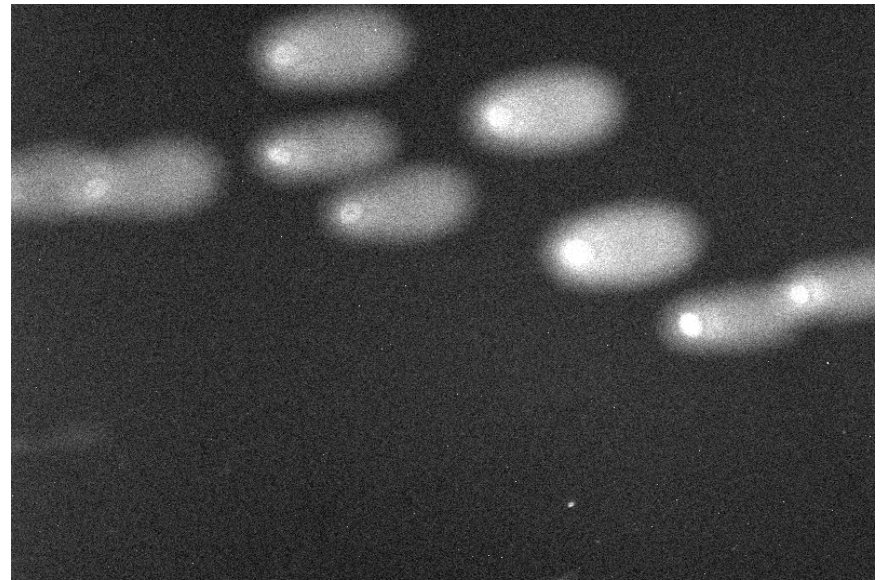


Figure 6. Comet tail images for DU145 cells

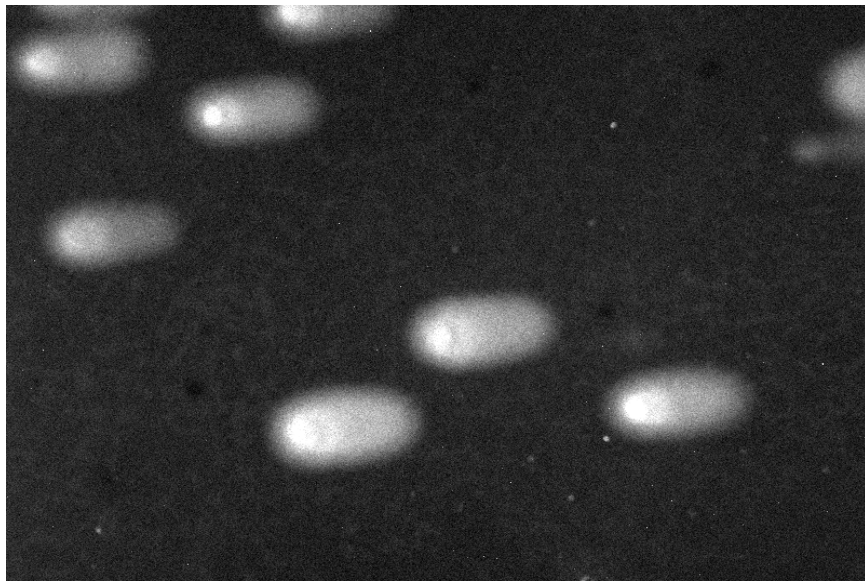
API (ABT888)



API (ABT888) +Rtx, 0min



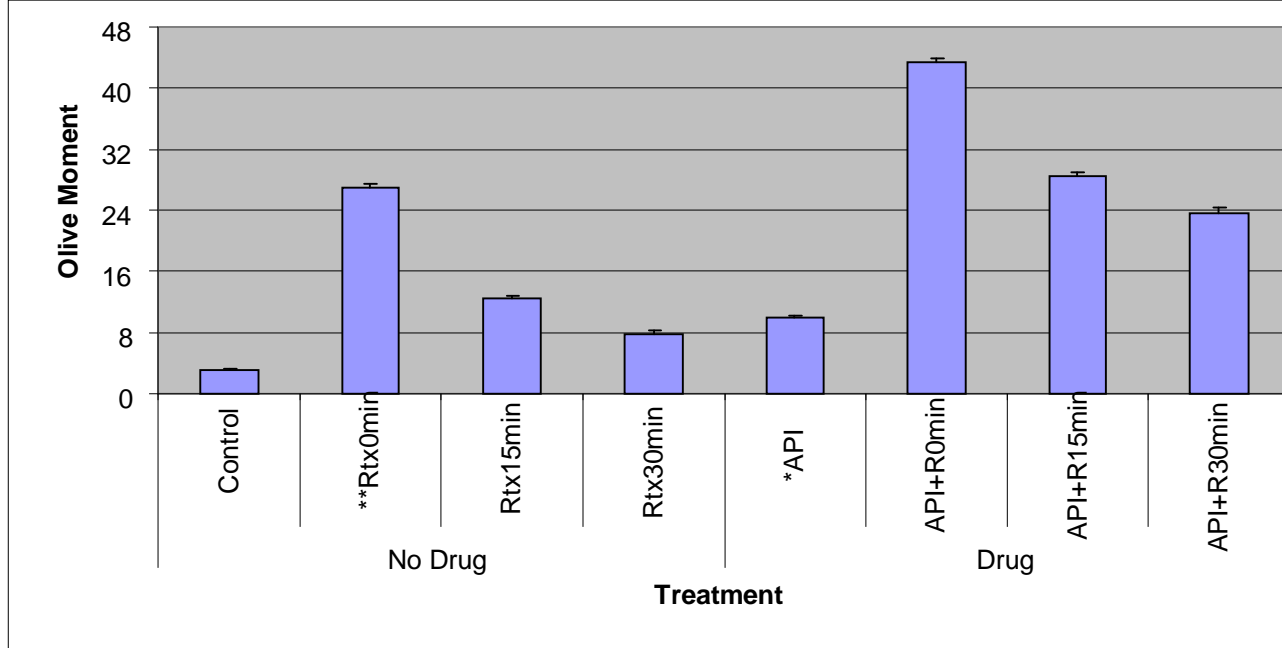
API (ABT888) +Rtx, 15min



API (ABT888) +Rtx, 30min



Figure 7. Comet tail images for DU145 cells.

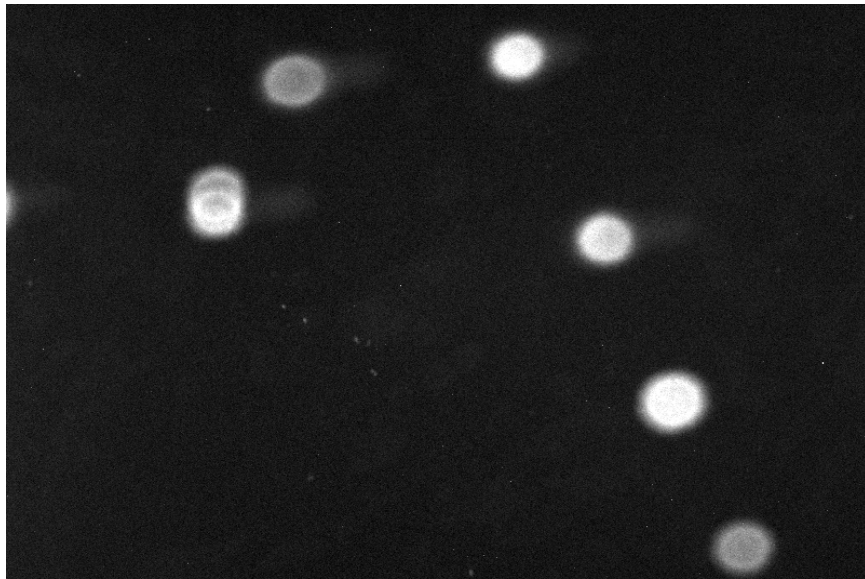


		N	Mean	Stdev	Stderr
No Drug	Control	40	3.05	1.62	0.256144
	Rtx0min	40	26.90	3.70	0.585021
	Rtx15min	51	12.42	3.01	0.421484
	Rtx30min	30	7.82	2.86	0.522162
Drug	API	61	9.96	2.36	0.302167
	API+R0min	38	43.39	2.98	0.48342
	API+R15min	60	28.51	4.37	0.564165
	API+R30min	37	23.64	4.77	0.784183

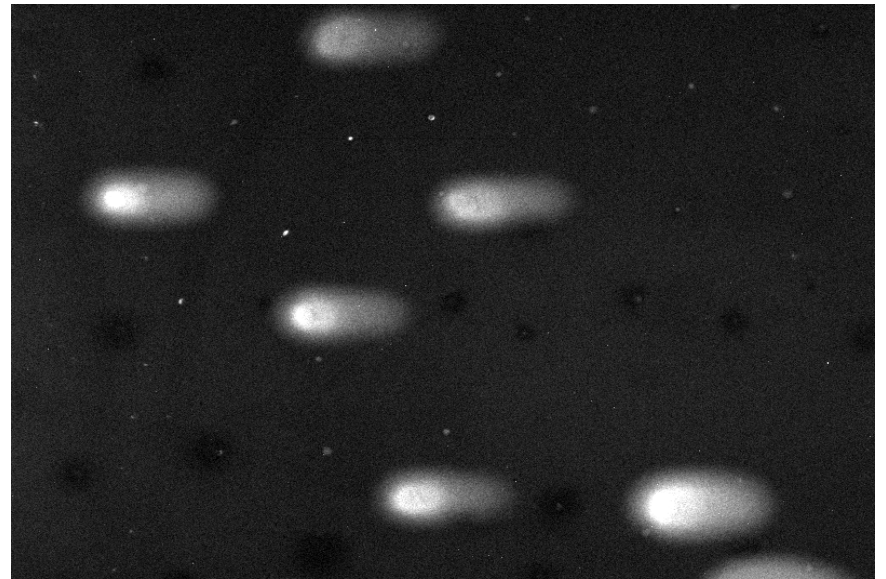
Figure 8. Comet Assay. Quantification of olive moment as a measure of kinetics of DNA repair in PC-3 cells.

***API = Abbott PARP Inhibitor (ABT888 (50 μ M); Rtx = **radiation (15 Gy)**

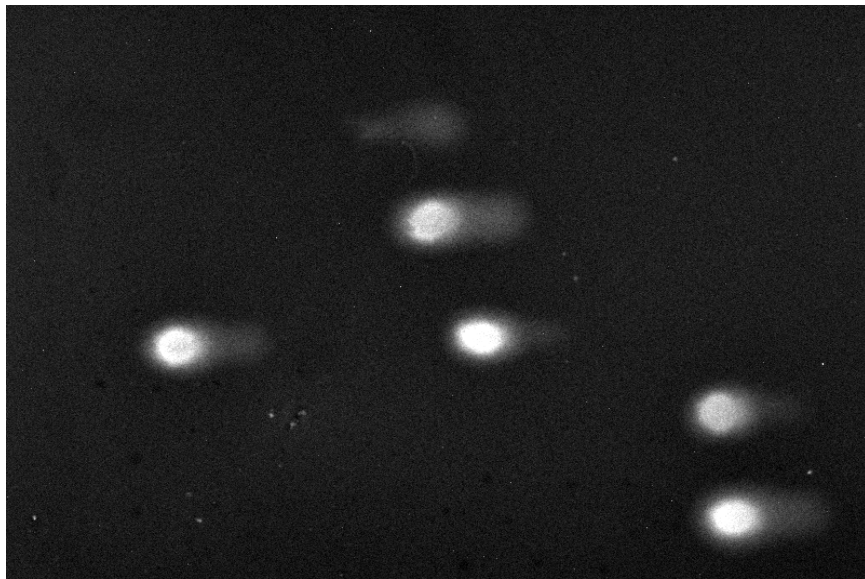
Control



Rtx, 0min



Rtx, 15min



Rtx, 30min

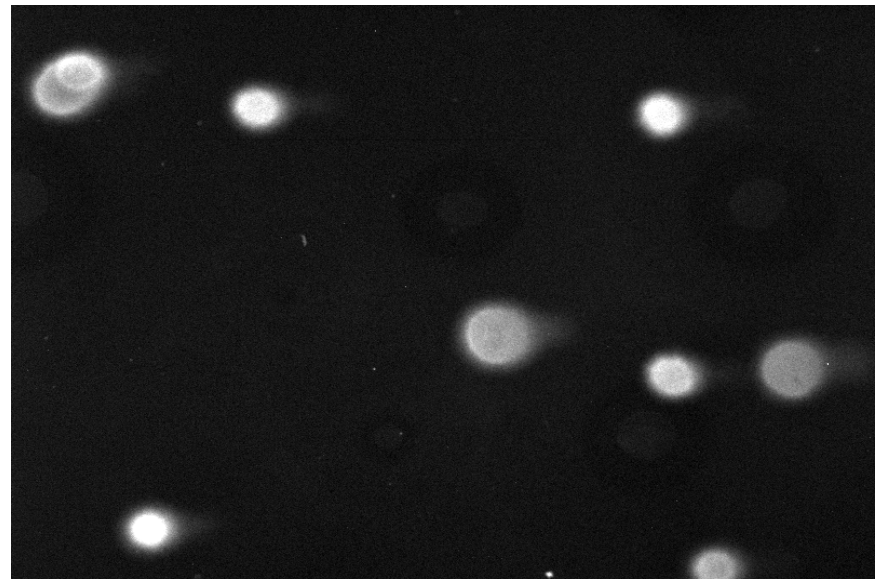
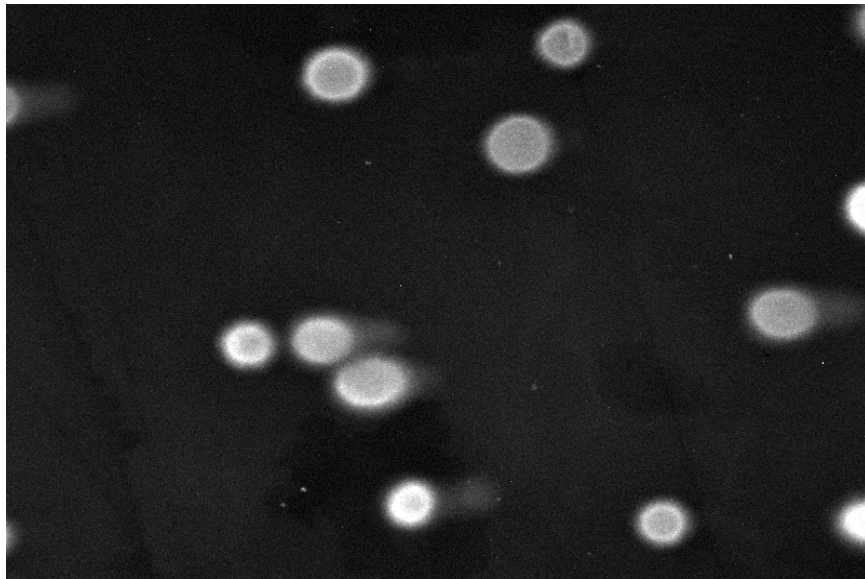
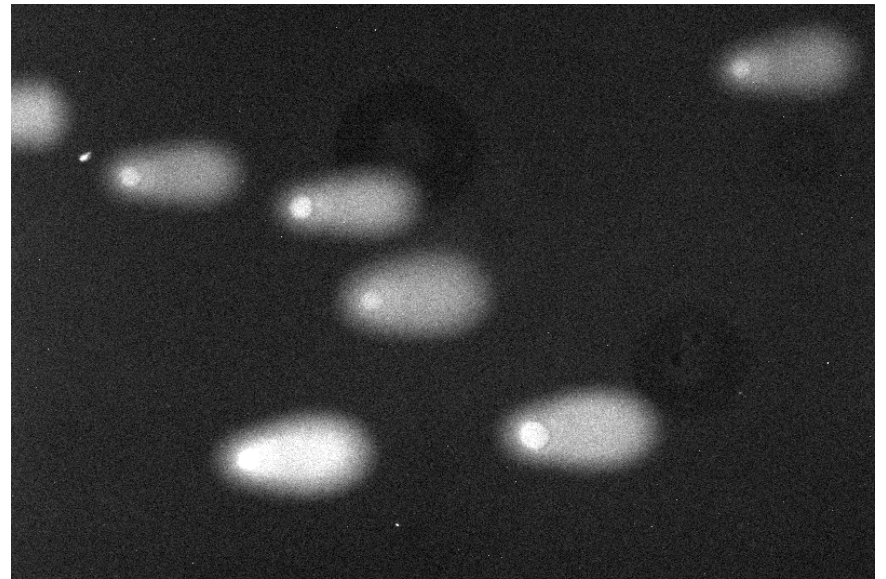


Figure 9. Comet tail images for PC-3 cells.

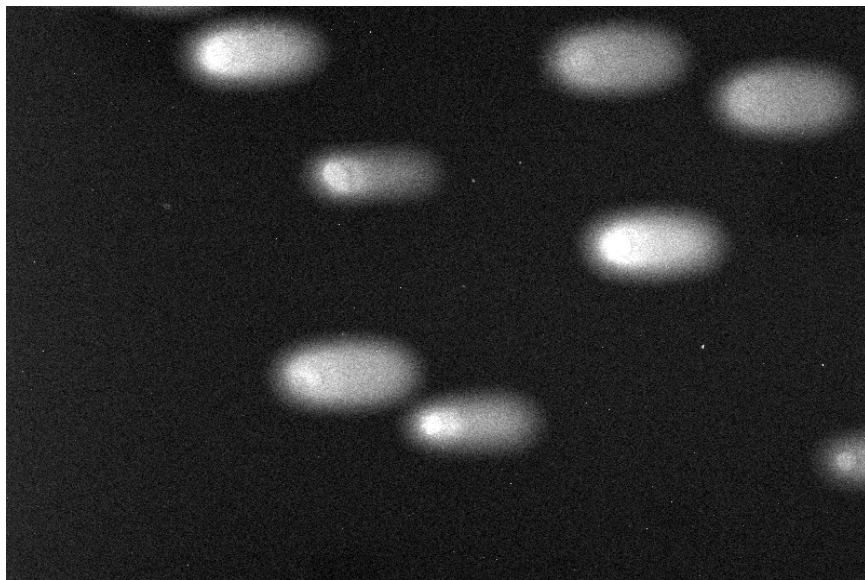
API (ABT888)



API (ABT888) +Rtx, 0min



API (ABT888) +Rtx, 15min



API (ABT888) +Rtx, 30min

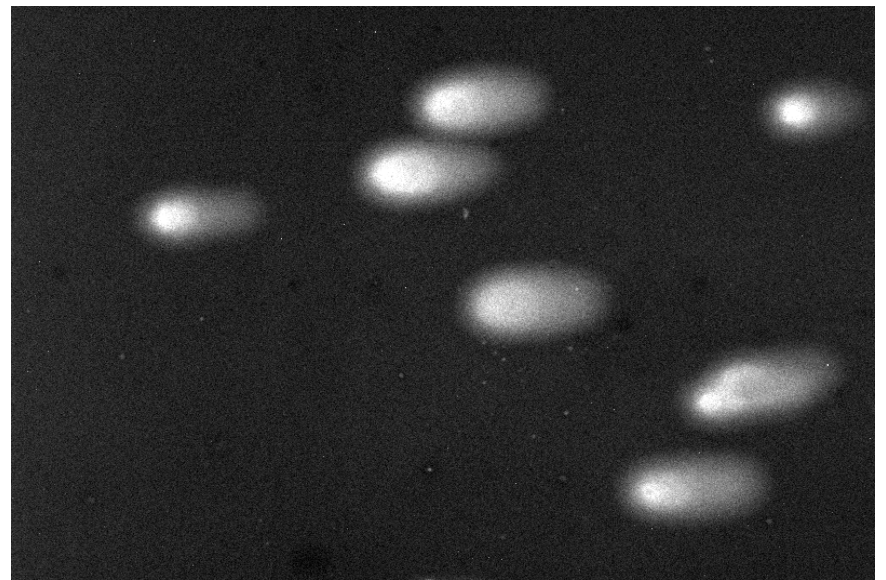
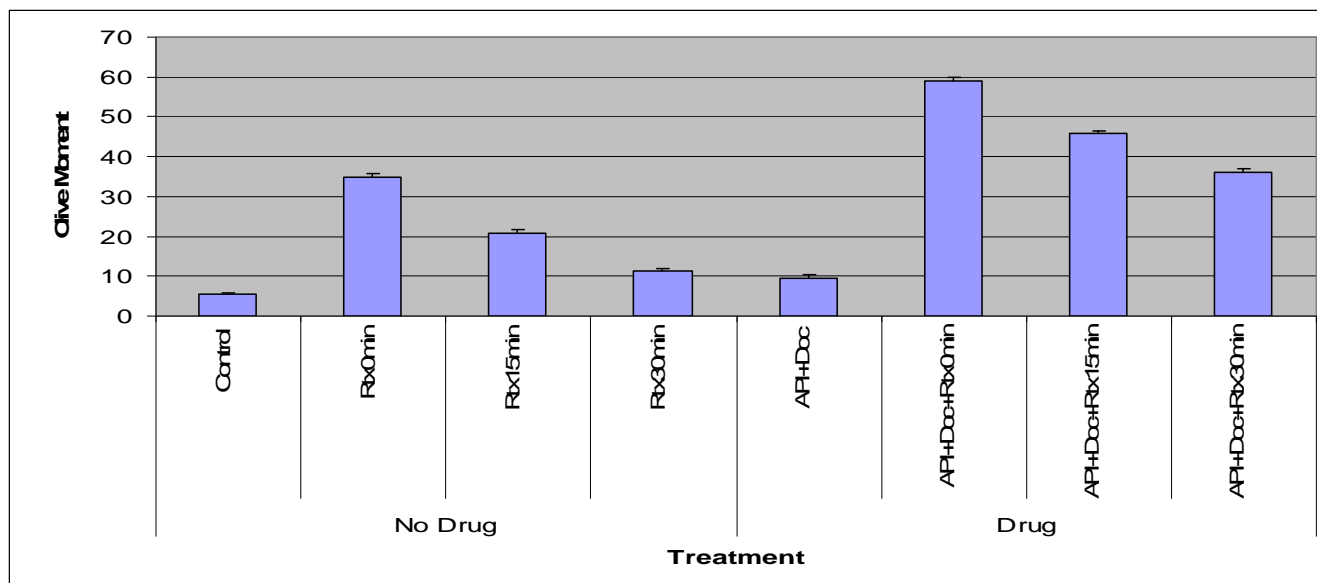


Figure 10. Comet tail images for PC-3 cells

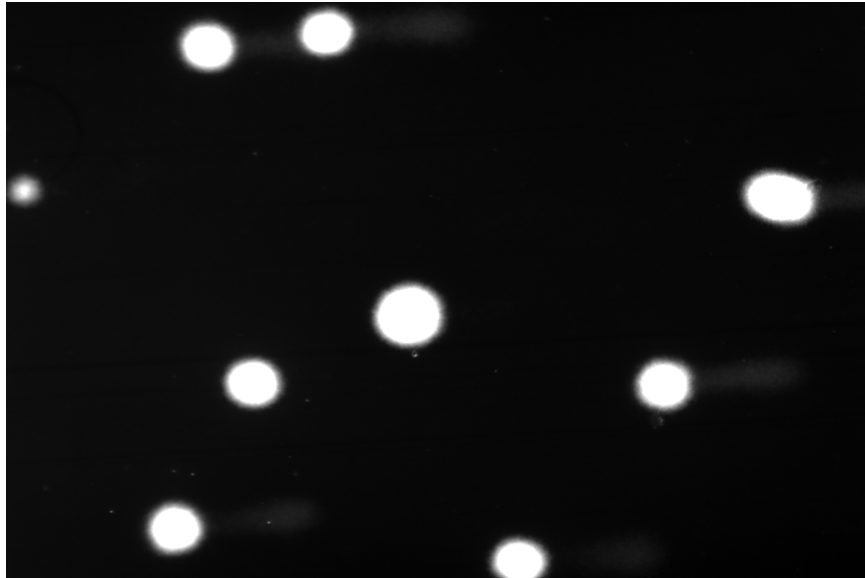


		N	Mean	Stdev	Stderr
No Drug	Control	60	5.41	2.38	0.307257
	Rtx0min	58	34.94	5.68	0.745821
	Rtx15min	50	20.84	6.89	0.974393
	Rtx30min	56	11.30	4.84	0.646772
Drug	API+Doc	45	9.49	5.25	0.782624
	API+Doc+Rtx0min	42	59.09	4.79	0.739113
	API+Doc+Rtx15min	48	45.84	5.19	0.749112
	API+Doc+Rtx30min	69	35.95	7.72	0.929379

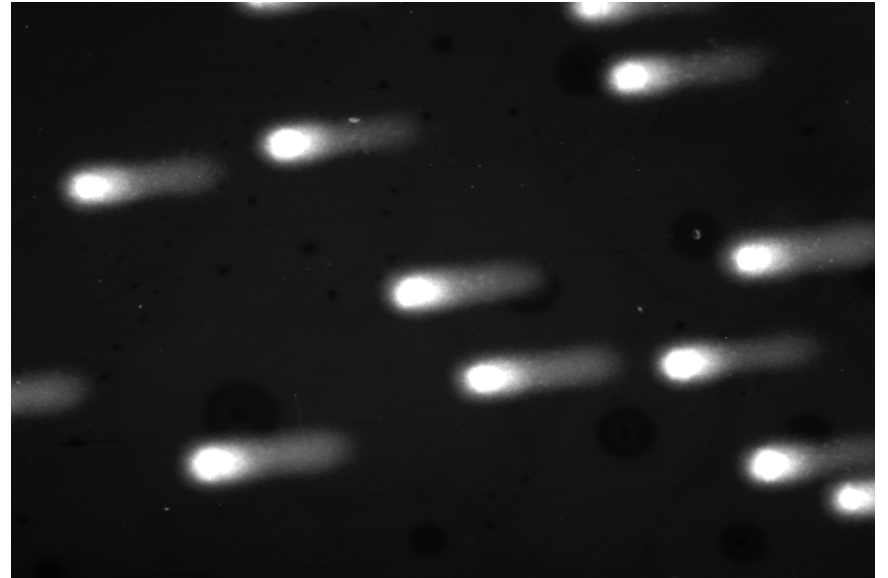
Figure 11. Comet Assay. Quantification of olive moment as a measure of kinetics of DNA repair in DU145 cells.

***API = Abbott PARP Inhibitor (ABT888 (50 μ M); Rtx = **radiation (15 Gy); Doc = docetaxel (5 nM).**

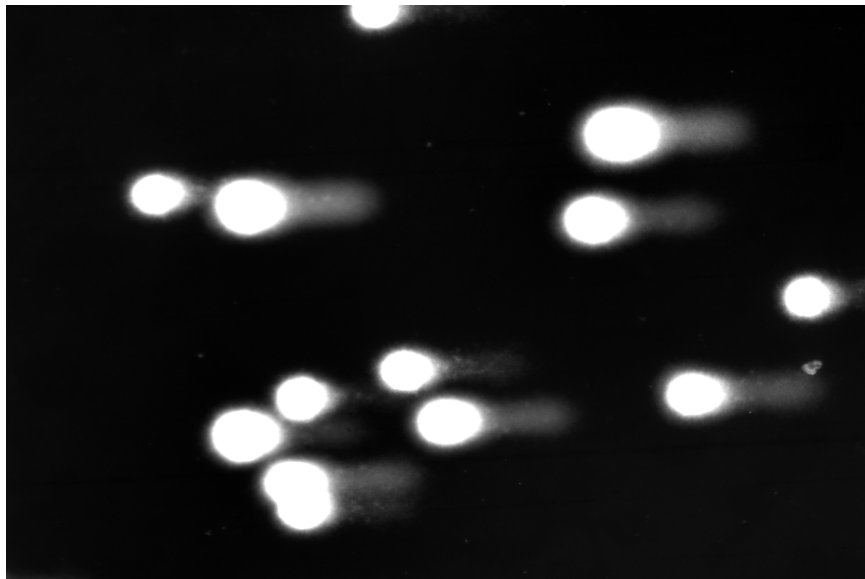
Control



Rtx, 0min



Rtx, 15min



Rtx, 30min

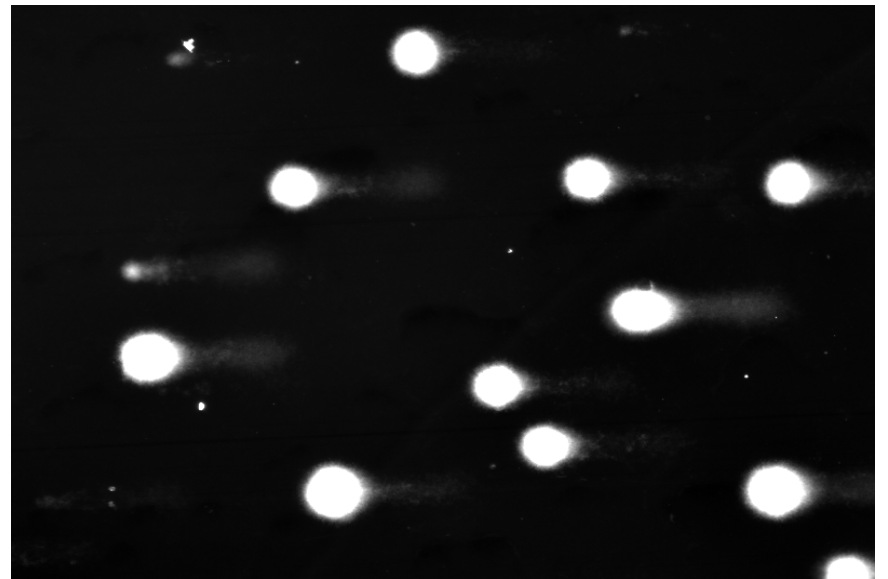
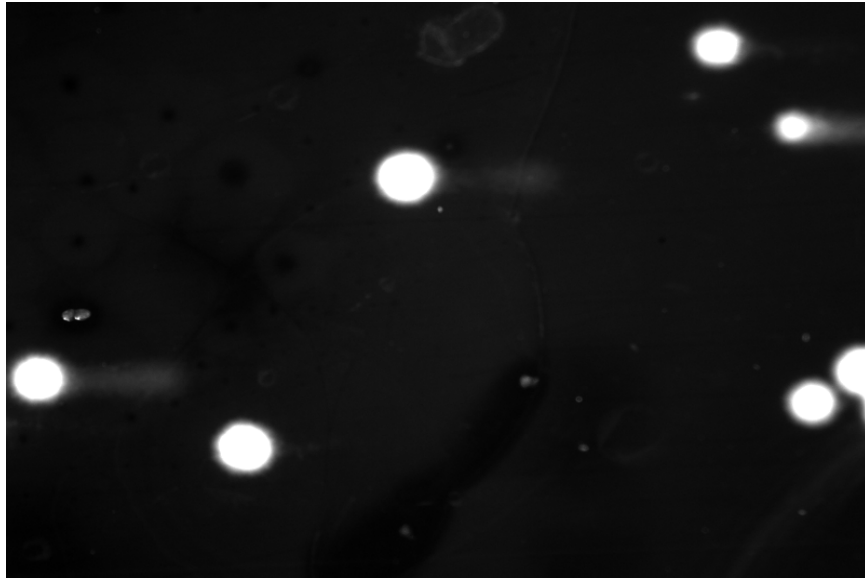
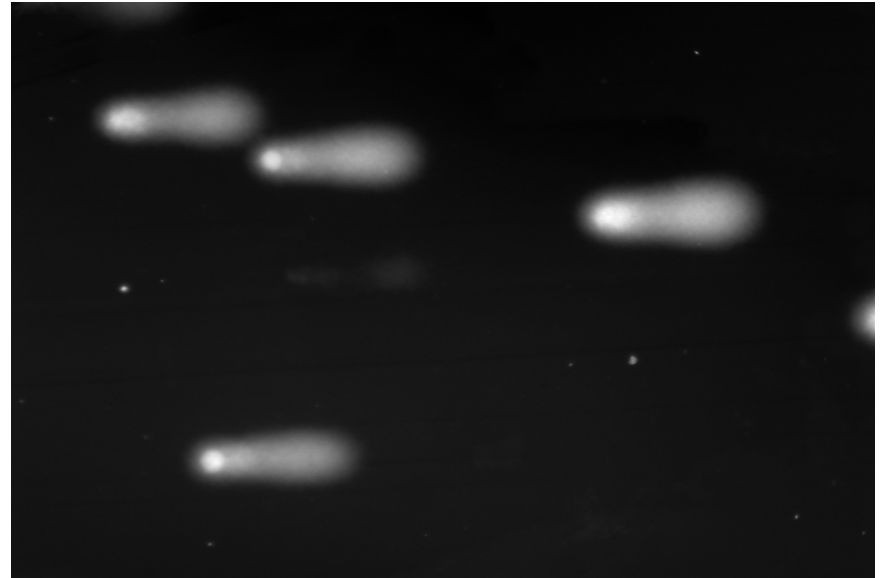


Figure 12. Comet tail images for DU145 cells

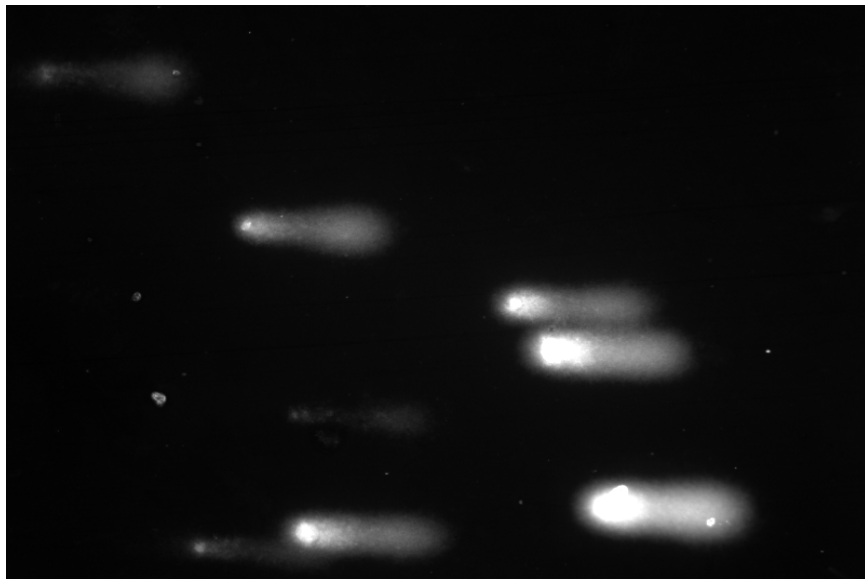
API+Doc



API+Doc+Rtx, 0min



API+Doc+Rtx, 15min



API+Doc+Rtx, 30min

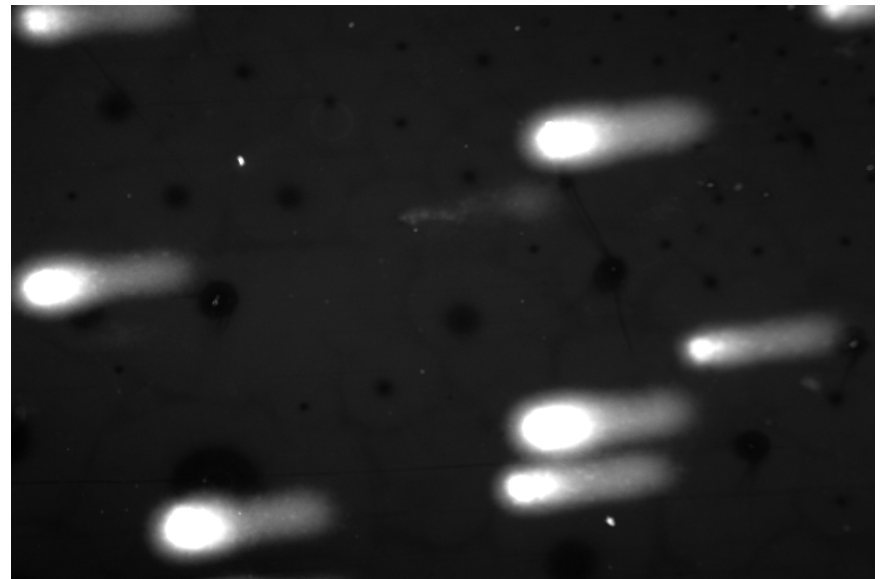
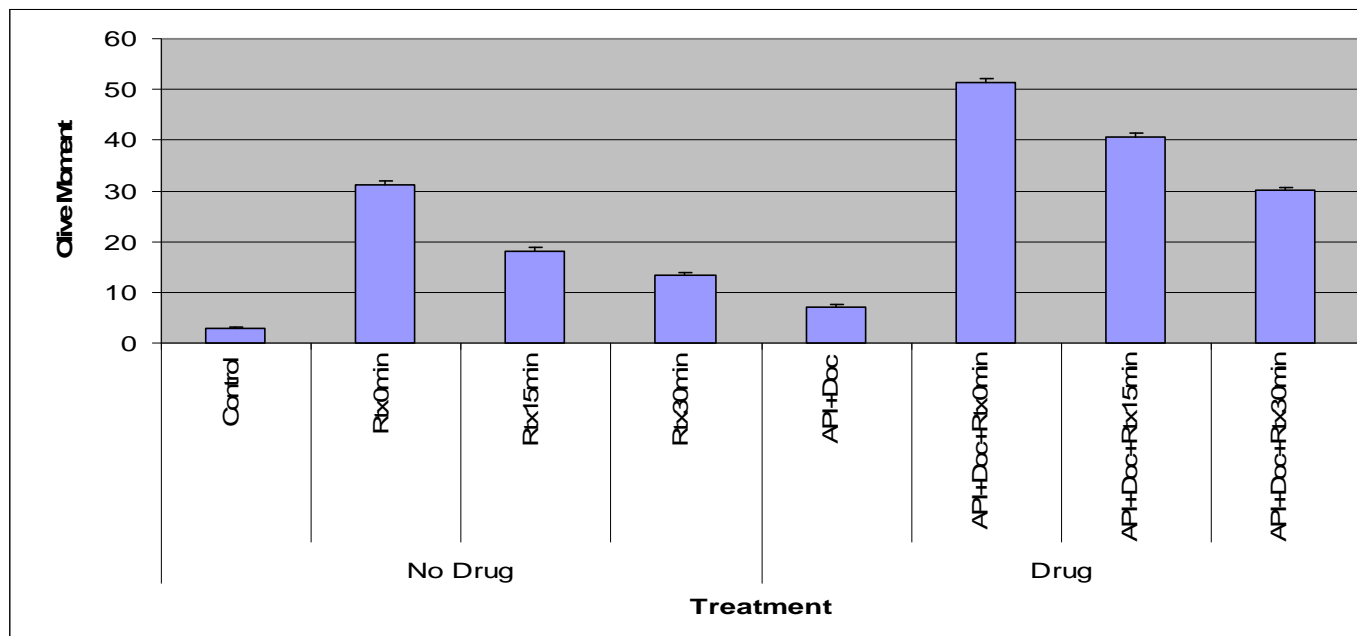


Figure 13. Comet tail images for DU145 cells

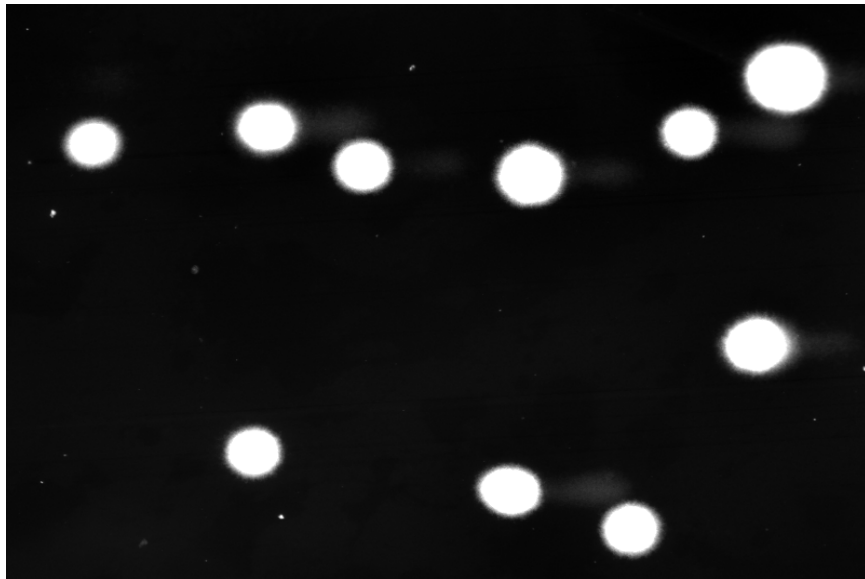


		N	Mean	Stdev	Stderr
No Drug	Control	64	2.84	1.99	0.24875
	Rtx0min	56	31.30	4.67	0.624055
	Rtx15min	63	18.13	5.13	0.646319
	Rtx30min	56	13.31	4.27	0.570603
Drug	API+Doc	43	7.05	4.00	0.609994
	API+Doc+Rtx0min	45	51.38	5.71	0.851197
	API+Doc+Rtx15min	44	40.73	4.28	0.645234
	API+Doc+Rtx30min	41	30.16	3.79	0.591899

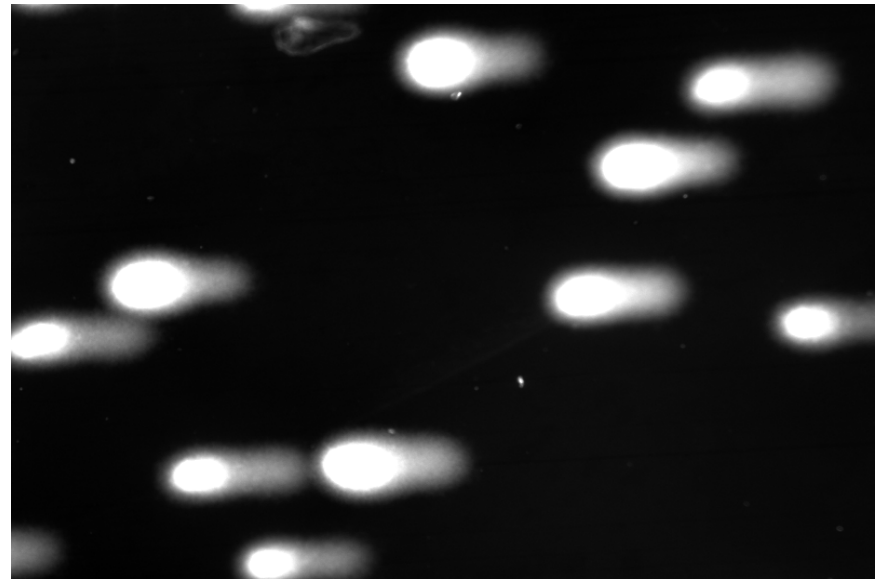
Figure 14. Comet Assay. Quantification of olive moment as a measure of kinetics of DNA repair in PC-3 cells.

***API = Abbott PARP Inhibitor (ABT888 (50 μ M); Rtx = **radiation (15 Gy); Doc = docetaxel (5 nM).**

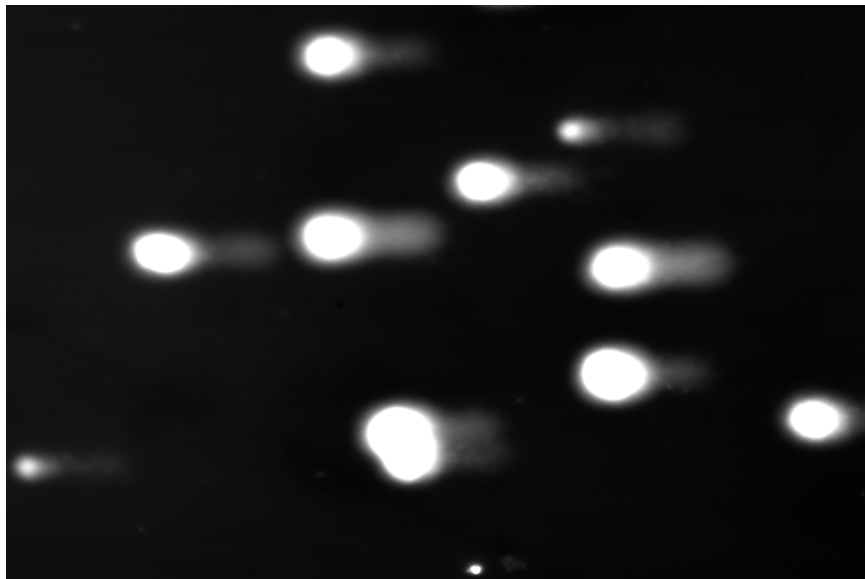
Control



Rtx, 0min



Rtx, 15min



Rtx, 30min

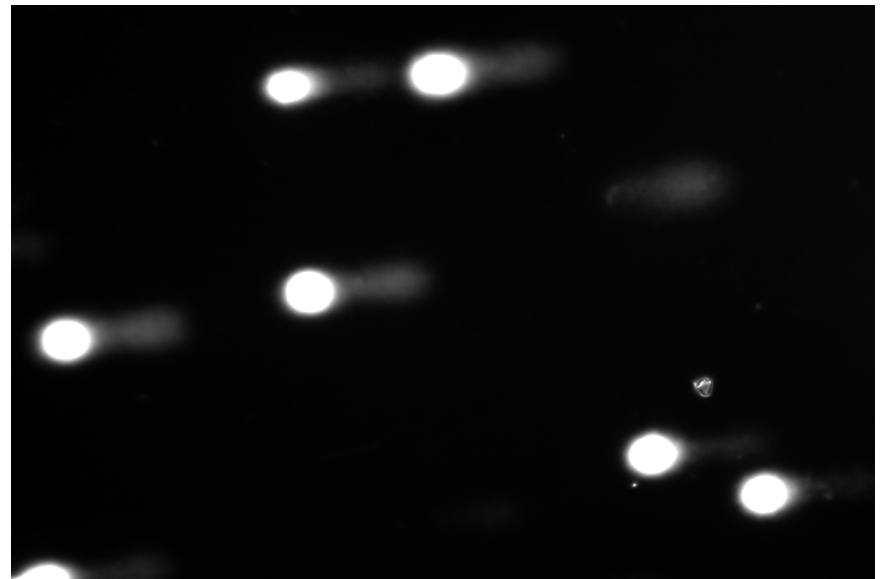
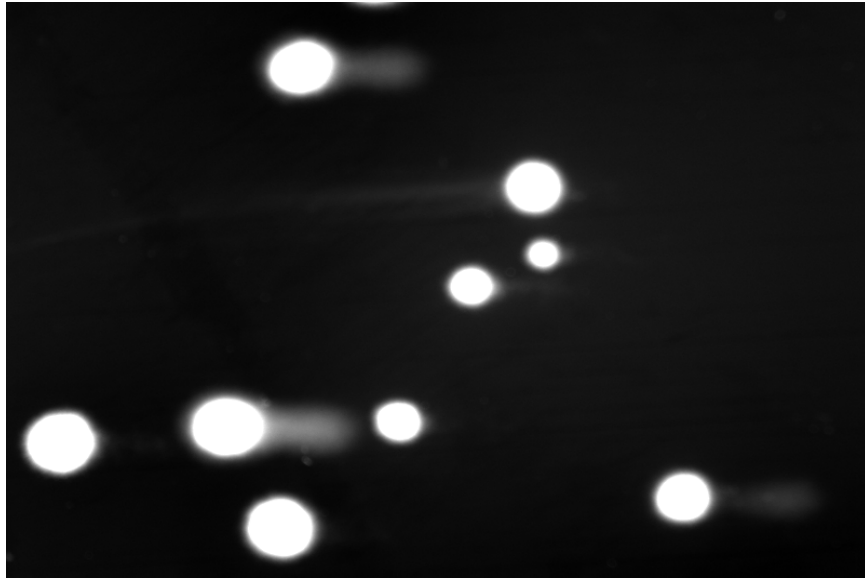
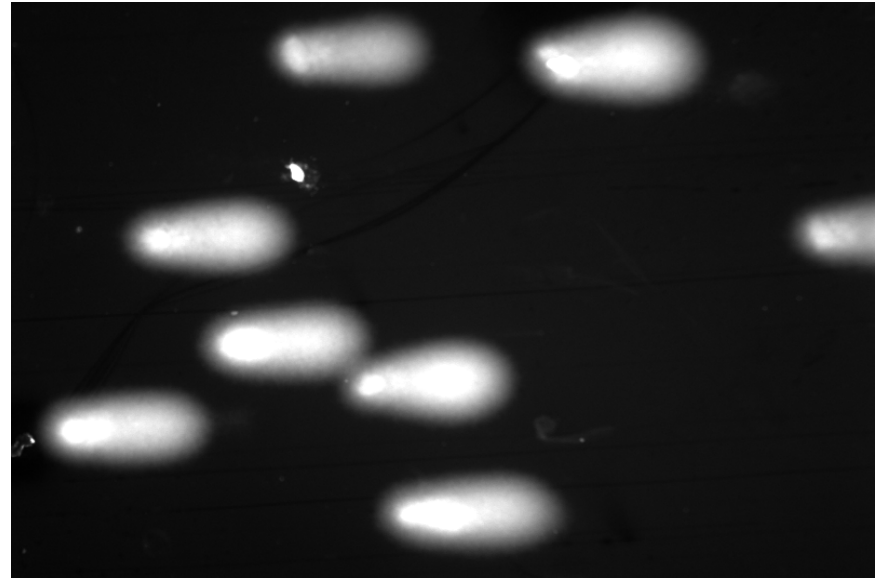


Figure 15. Comet tail images for PC-3 cells

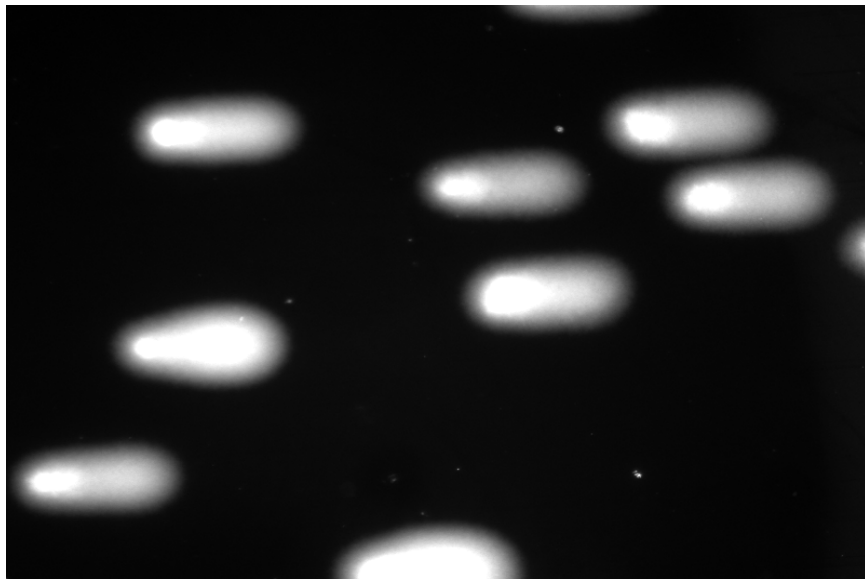
API+Doc



API+Doc+Rtx, 0min



API+Doc+Rtx, 15min



API+Doc+Rtx, 30min

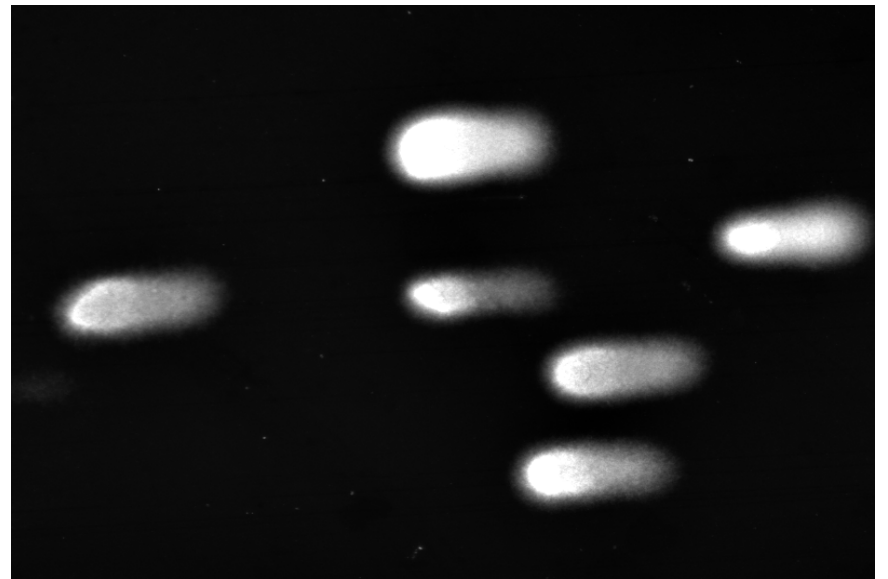
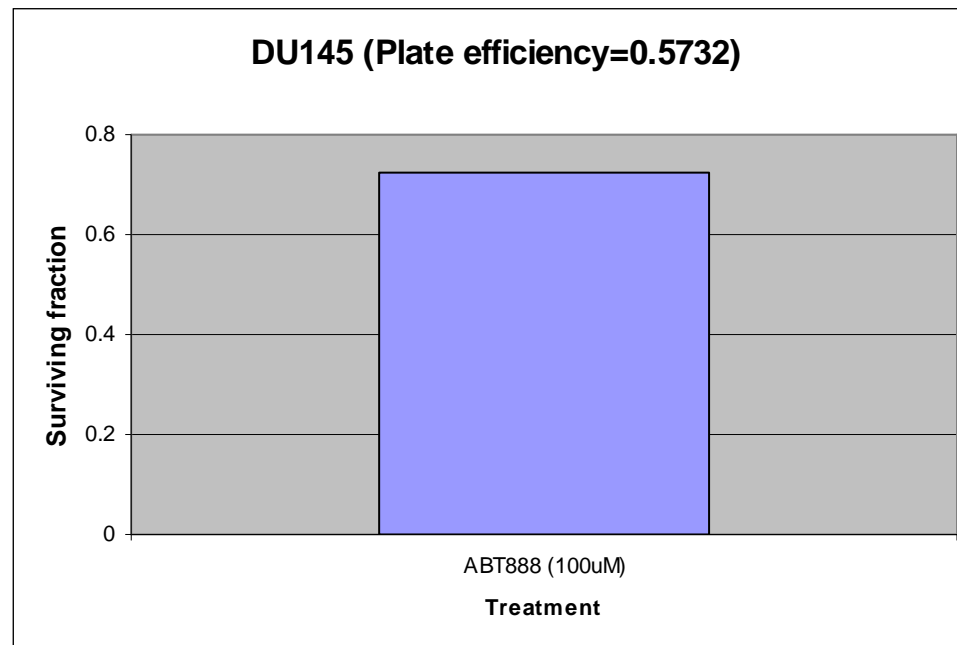
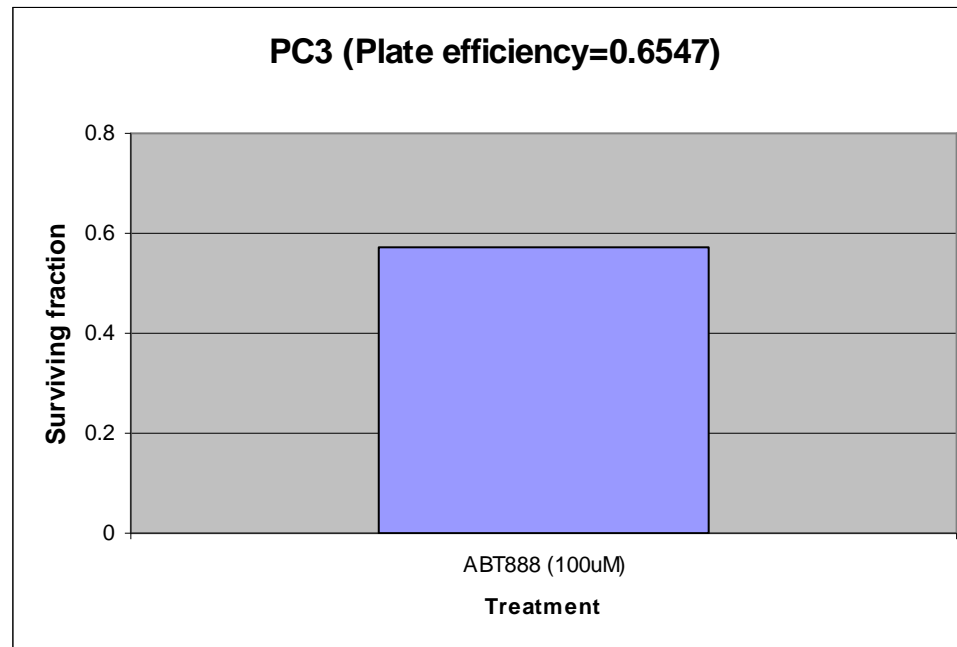


Figure 16. Comet tail images for PC-3 cells

Figure 17. Clonogenic cell Survival after treatment with ABT888 for 24 hr in PC-3 And DU145 cells.



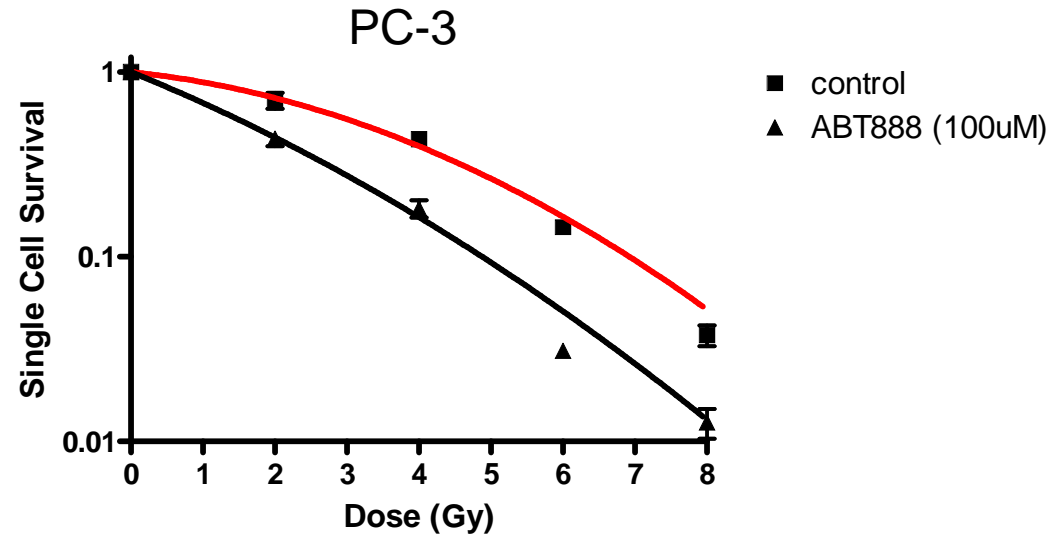
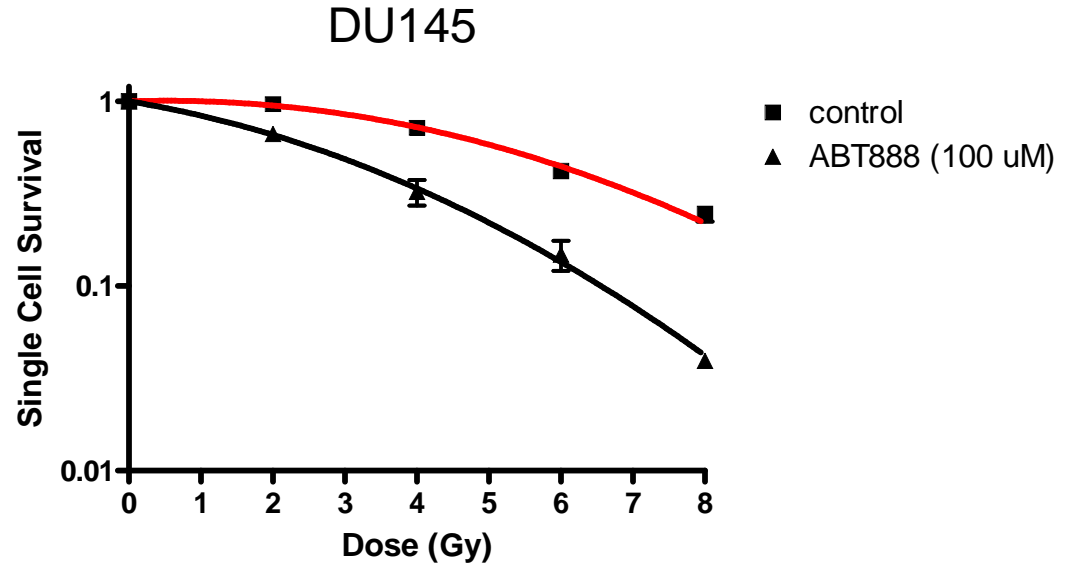
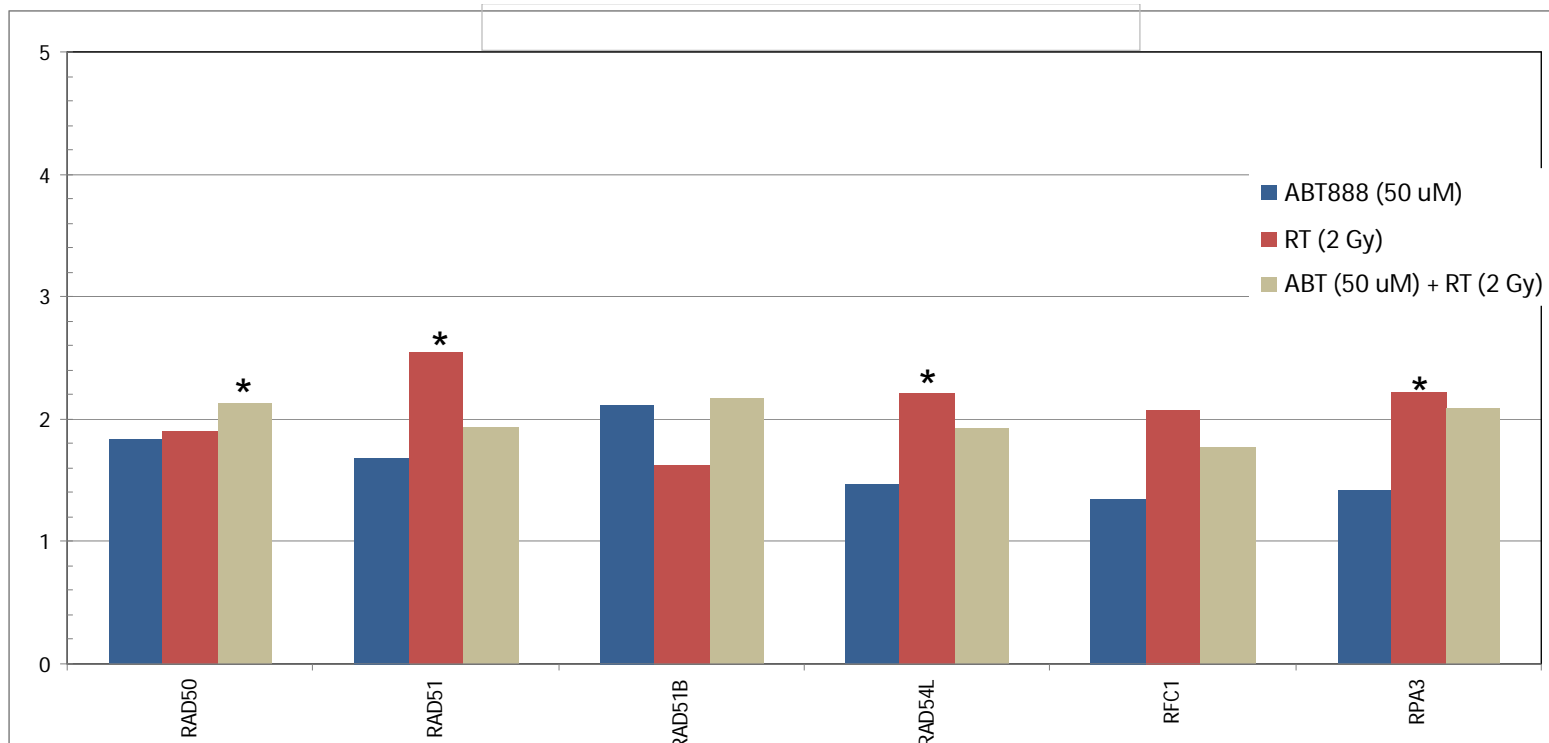


Figure 18. Clonogenic cell survival in DU145 and PC-3 cells after treatment with ABT888 for 24 hr.

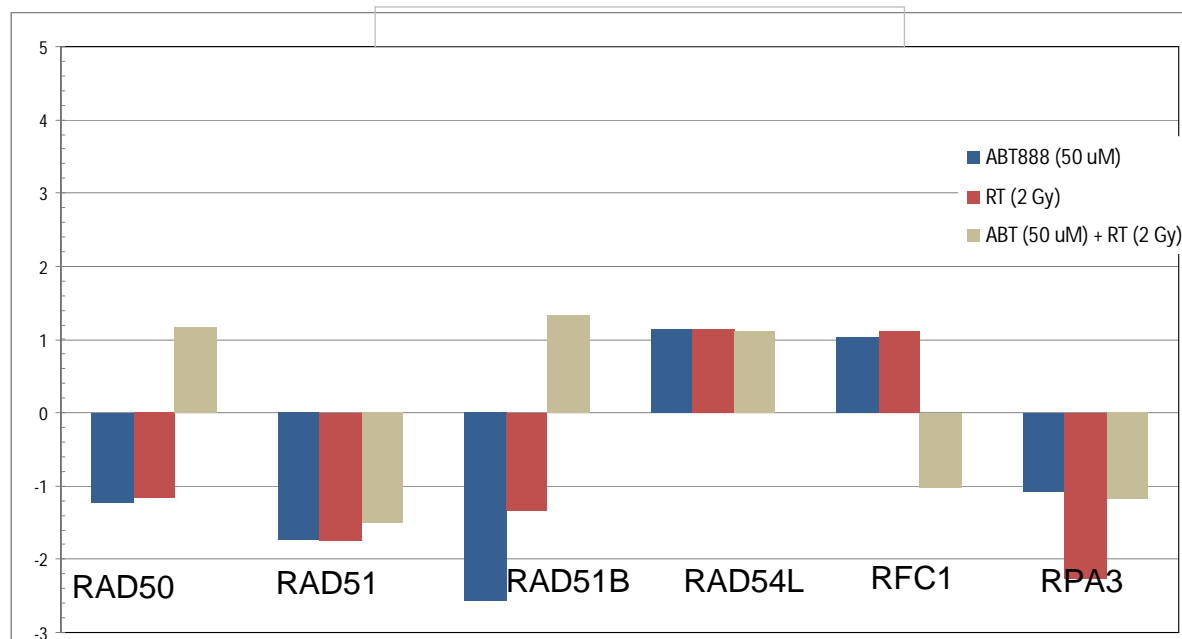
Up- Regulation of PC3 cells (Compared to Control Group) at 24 hr



		PC3 24 hr Up-Down Regulation (comparing to control group)			p-value (comparing to control group)		
		ABT888 (50 uM)	RT (2 Gy)	ABT (50 uM) + RT (2 Gy)	ABT888 (50 uM)	RT (2 Gy)	ABT (50 uM) + RT (2 Gy)
		Fold Regulation	Fold Regulation	Fold Regulation	p-value	p-value	p-value
E10	RAD50	1.8404	1.8956	2.1254	0.145291	0.23242	0.005039
E11	RAD51	1.6854	2.5438	1.9322	0.238626	0.03727	0.066692
E12	RAD51B	2.1139	1.6164	2.1715	0.117647	0.184823	0.226385
F04	RAD54L	1.4692	2.2153	1.9195	0.061793	0.015517	0.213384
F05	RFC1	1.3536	2.0785	1.7686	0.132958	0.066939	0.294033
F07	RPA3	1.4144	2.2286	2.0879	0.137213	0.040285	0.149383

Figure 19. Fold regulation of DNA repair genes 24 hr following ABT888 and/or 2 Gy treatment in PC-3 (PTEN null) cells (a). Out of 87 genes, in a DNA repair panel (SABiosciences) 6 genes were selected based upon the magnitude of up or down regulation with a ≥ 2 -fold cutoff within at least one of the treatment conditions. * = p value < 0.05.

Up-Down Regulation of DU145 cells (Compared to Control Group) at 24 hr



		DU145 24 hr Up-Down Regulation (comparing to control group)			p-value (comparing to control group)		
		ABT888 (50 uM)	RT (2 Gy)	ABT (50 uM) + RT (2 Gy)	ABT888 (50 uM)	RT (2 Gy)	ABT (50 uM) + RT (2 Gy)
		Fold Regulation	Fold Regulation	Fold Regulation	p-value	p-value	p-value
E10	RAD50	-1.2158	-1.1511	1.1766	0.485544	0.78494	0.562133
E11	RAD51	-1.7302	-1.7486	-1.5005	0.265796	0.248953	0.398027
E12	RAD51B	-2.5732	-1.327	1.3348	0.182962	0.321612	0.485549
F04	RAD54L	1.1445	1.1479	1.1217	0.6138	0.640725	0.678973
F05	RFC1	1.0376	1.1192	-1.0179	0.870261	0.588309	0.999875
F07	RPA3	-1.0656	-2.2592	-1.1754	0.645641	0.157057	0.403315

Figure 20. Fold regulation of DNA repair genes 24 hr following ABT888 and/or 2 Gy treatment in DU145 (PTEN wt) cells (a). Genes were selected based on those selected for PC-3 analysis in Figure 18. No fold differences reached significance.

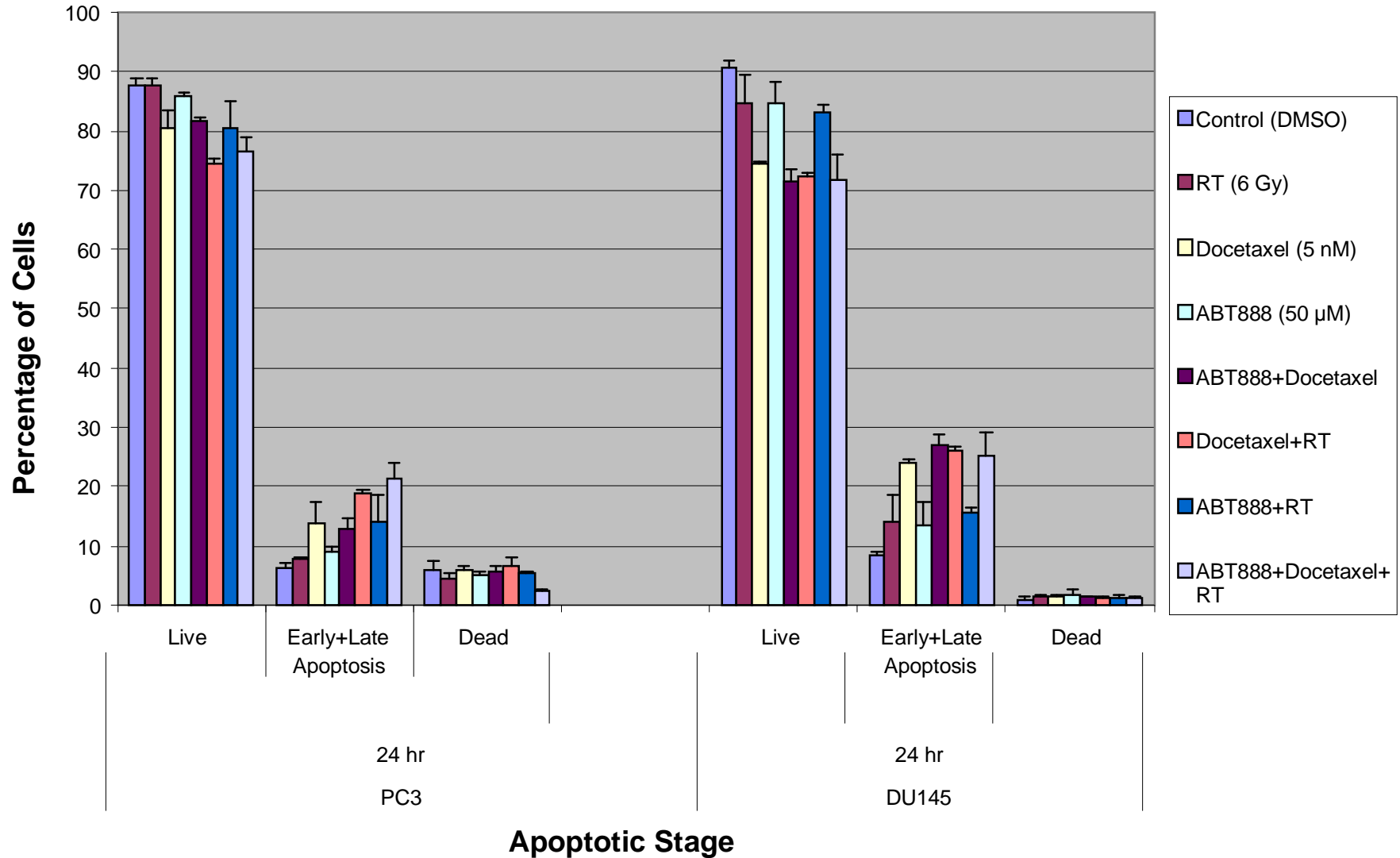


Figure 21. Effect of ABT888, Docetaxel and/or RT on induction of apoptosis in DU145 and PC-3 cells. The mean \pm SEM from at least two independent experiments were obtained with three replicates per experiment.

Treatment	*Apoptosis	
	DU145	PC-3
Control (DMSO vehicle)	8.3	6.4
RT	14.1	7.7
Docetaxel	24.1	13.7
ABT888	13.5	9.1
ABT888+Docetaxel	27.1	12.7
Docetaxel+RT	26.2	18.9
ABT888+RT	15.5	14.1
ABT888+Docetaxel+RT	25.1	21.2

*percentage of cell population undergoing early and late apoptosis

Figure 22 Tabulation of percentage of cells undergoing early and late apoptosis

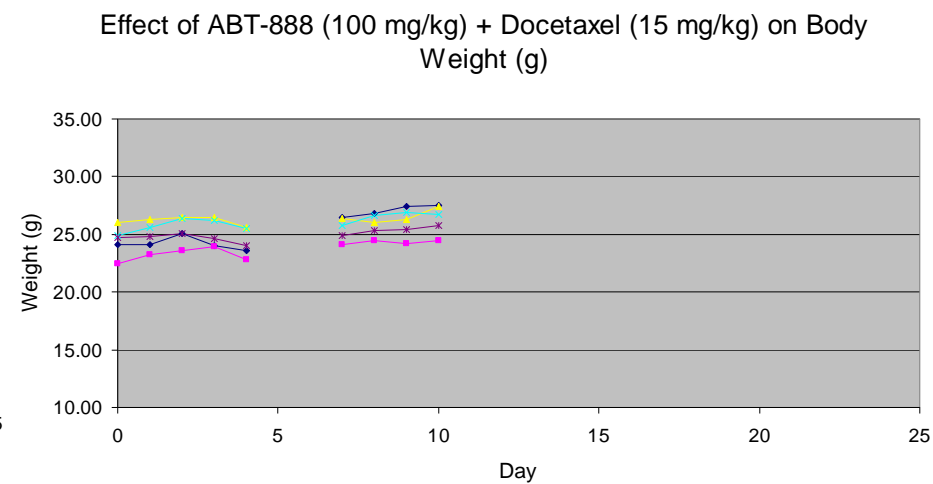
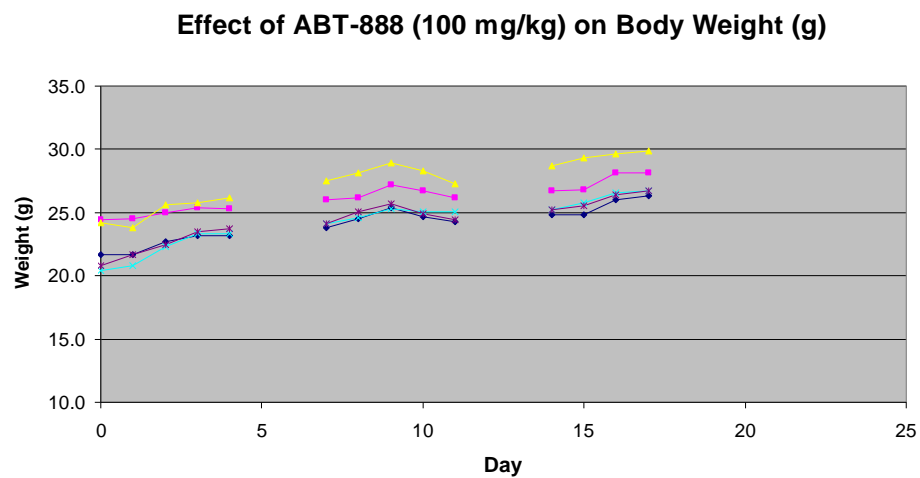
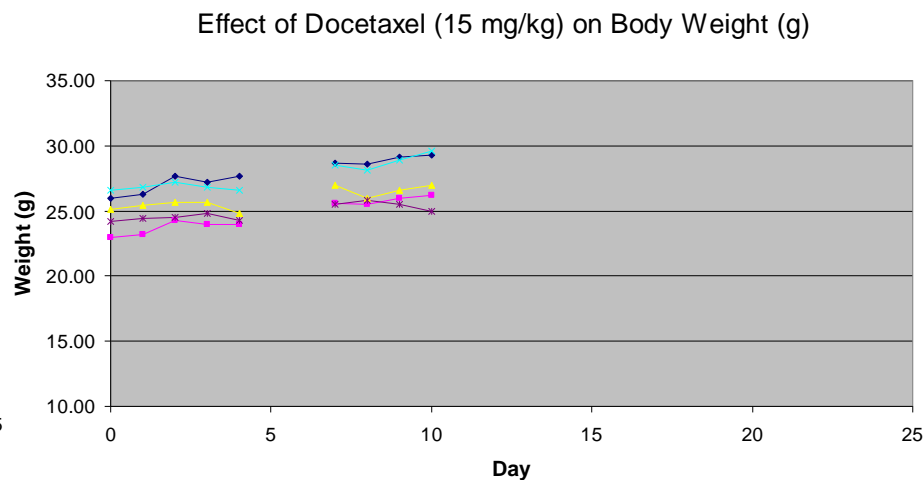
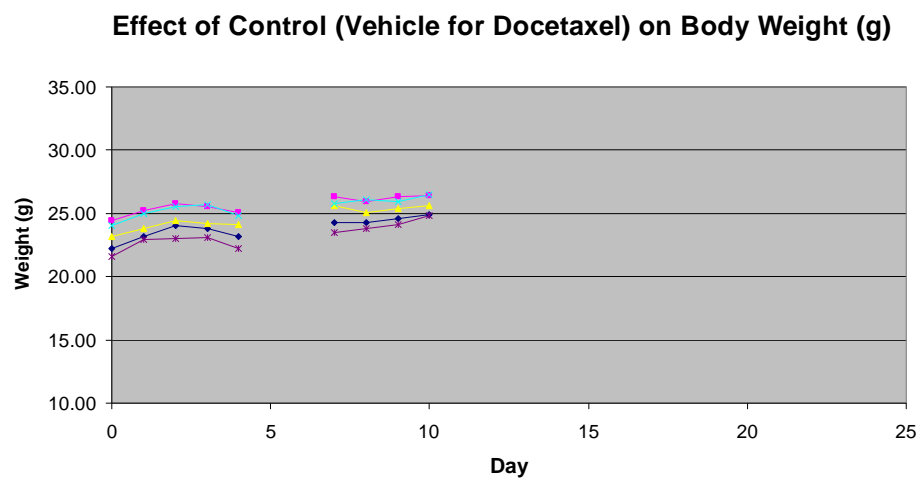


Figure 23. Effect of ABT888 and Docetaxel on non-tumored animals. (N=5 animals per treatment)

DU145 xenografts

Table 1. Number of animals (n) and number of tumor measurements per animal by treatment group.

Group	N	Mean	Range
Control	12	29.33	11-38
Docetaxel	7	23.86	4-41
RTX alone	11	31.18	11-38
ABT-888	11	24	4-41
Docetaxel+RTX	9	26.67	4-40
ABT-888+ Docetaxel	6	23	4-39
ABT-888 + RTX	14	29.21	4-41
ABT-888+ Docetaxel + RTX	9	27.22	5-41

Table 2. Estimates of geometric mean tumor volume over time by treatment group.

	Tumor volume				
	<i>Time (days)</i>				
	<i>0</i>	<i>14</i>	<i>28</i>	<i>42</i>	<i>56</i>
Control	140.72	282.39	566.68	1137.17	2282
Docetaxel	220.11	331.59	499.54	752.54	1133.68
RTX alone	105.5	179.79	306.38	522.12	889.75
ABT-888	167.6	235.41	330.66	464.45	652.38
Docetaxel+RTX	175.89	260.79	386.66	573.29	850
ABT-888+ Docetaxel	167.69	276.33	455.35	750.35	1236.47
ABT-888 + RTX	175.38	227.05	293.95	380.55	492.67
ABT-888+ Docetaxel + RTX	180.72	308.48	526.57	898.84	1534.28

DU145 xenografts

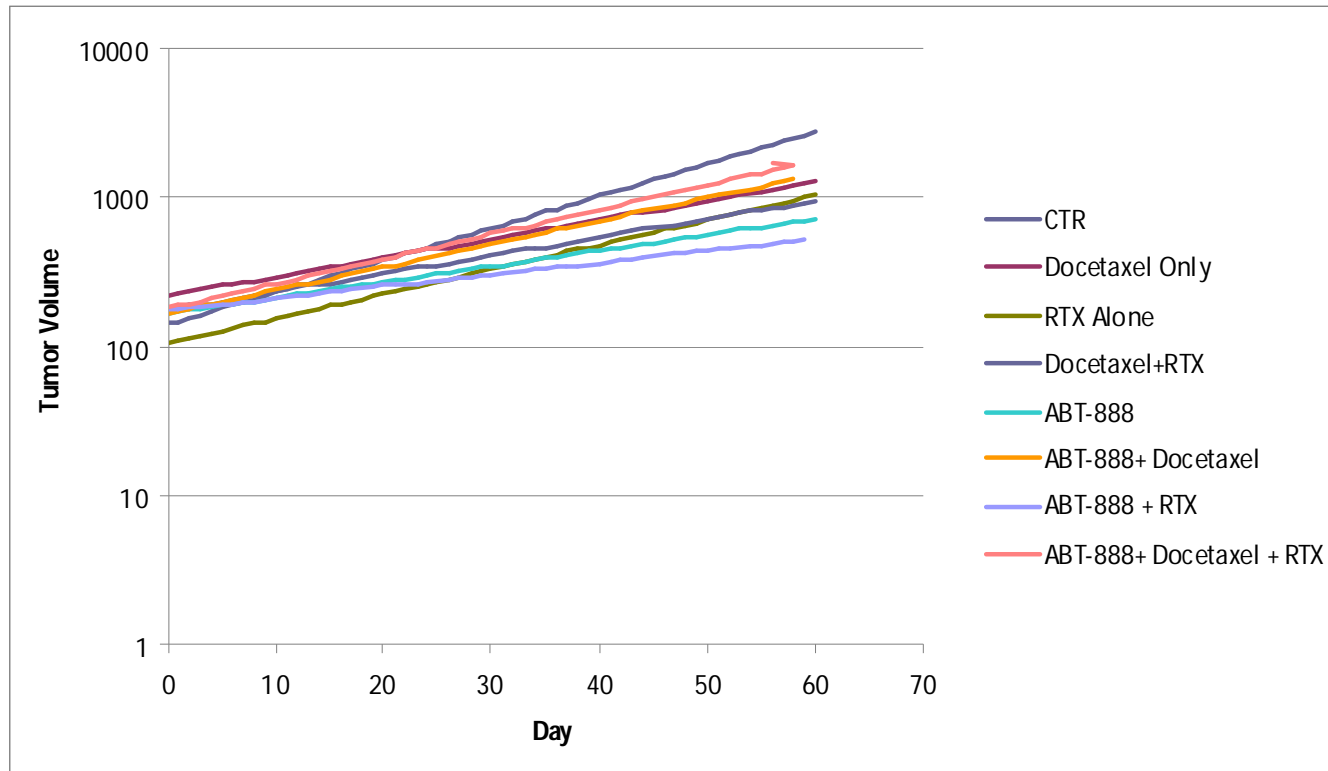


Figure 24. Model-estimated geometric mean tumor volume by group and time.

DU145 xenografts

Table 3. Tumor growth rate (% change in volume per day) by group

Group	%Δ Volume (95% CI)	Tumor Doubling Time (95% CI)
Control	5.1 (2.8 , 7.4)	13.9 (9.7 , 24.9)
Docetaxel	3 (-0.1 , 6.2)	23.7 (11.6 , *)
ABT-888	2.5 (0 , 5)	28.6 (14.3 , 25085.8)
RTX alone	3.9 (1.5 , 6.3)	18.2 (11.4 , 45.7)
Docetaxel+RTX	2.9 (0.2 , 5.6)	24.6 (12.7 , 443.3)
ABT-888+ Docetaxel	3.6 (0.2 , 7.2)	19.4 (9.9 , 428.2)
ABT-888 + RTX	1.9 (-0.3 , 4)	37.6 (17.5 , *)
ABT-888+ Docetaxel + RTX	3.9 (1.2 , 6.7)	18.1 (10.7 , 58.5)

%Δ: estimated average rate of increase of tumor volume (% daily change) $100 \times (\text{geometric mean ratio} - 1)$. *Tumor doubling time is a function of the rate of growth. When the 95% CI for the growth rate has a negative bound (i.e., tumor shrinkage may be consistent with the data), then the upper bound for tumor doubling time cannot be calculated.

Table 4. Comparison of Growth Rates

Group Comparison	p-value for comparison of growth rates
RTX Alone vs. CTR	0.46
ABT-888 vs. CTR	0.12
Docetaxel vs. CTR	0.28
ABT-888+RTX vs. ABT-888	0.72
ABT-888+RTX vs. RTX Alone	0.21
ABT-888+Docetaxel vs. ABT-888	0.59
ABT-888+Docetaxel vs. Docetaxel	0.78
Docetaxel+RTX vs Docetaxel	0.96
Docetaxel+RTX vs. RTX Alone	0.57
ABT-888+Docetaxel+RTX vs. ABT-888+ RTX	0.25
ABT-888+Docetaxel+RTX vs. ABT-888+ Docetaxel	0.91
ABT-888+Docetaxel+RTX vs. Docetaxel+RTX	0.59

PC-3 xenografts

Table 5. Number of animals (n) and number of tumor measurements per animal by treatment group.

Group	N	Mean	Range
Control	12	20.5	4-40
Docetaxel	10	28	4-41
RTX alone	13	28.46	4-40
Docetaxel+RTX	10	27.8	4-40
ABT	13	26.46	4-41
ABT+ Docetaxel	8	22.13	3-41
ABT + RTX	9	23.67	4-40
ABT+ Docetaxel + RTX	11	29.55	4-40

Table 6. Estimates of geometric mean tumor volume over time by treatment group.

	Tumor volume				
	<i>Time (days)</i>				
	<i>0</i>	<i>14</i>	<i>28</i>	<i>42</i>	<i>56</i>
Control	191.12	551.39	1590.83	4589.69	13241.74
Docetaxel	205.29	328.92	527.01	844.4	1352.93
RTX alone	203.09	331.73	541.87	885.13	1445.83
Docetaxel+RTX	207.49	309.64	462.08	689.56	1029.04
ABT-888	221.10	496.74	1116.03	2507.39	5633.38
ABT-888+ Docetaxel	184.49	432.48	1013.83	2376.63	5571.31
ABT-888 + RTX	179.83	242.91	328.12	443.21	598.68
ABT-888+ Docetaxel + RTX	185.17	255.46	352.43	486.2	670.76

Note: italicized values are beyond the range of the observed volume data.

PC-3 xenografts

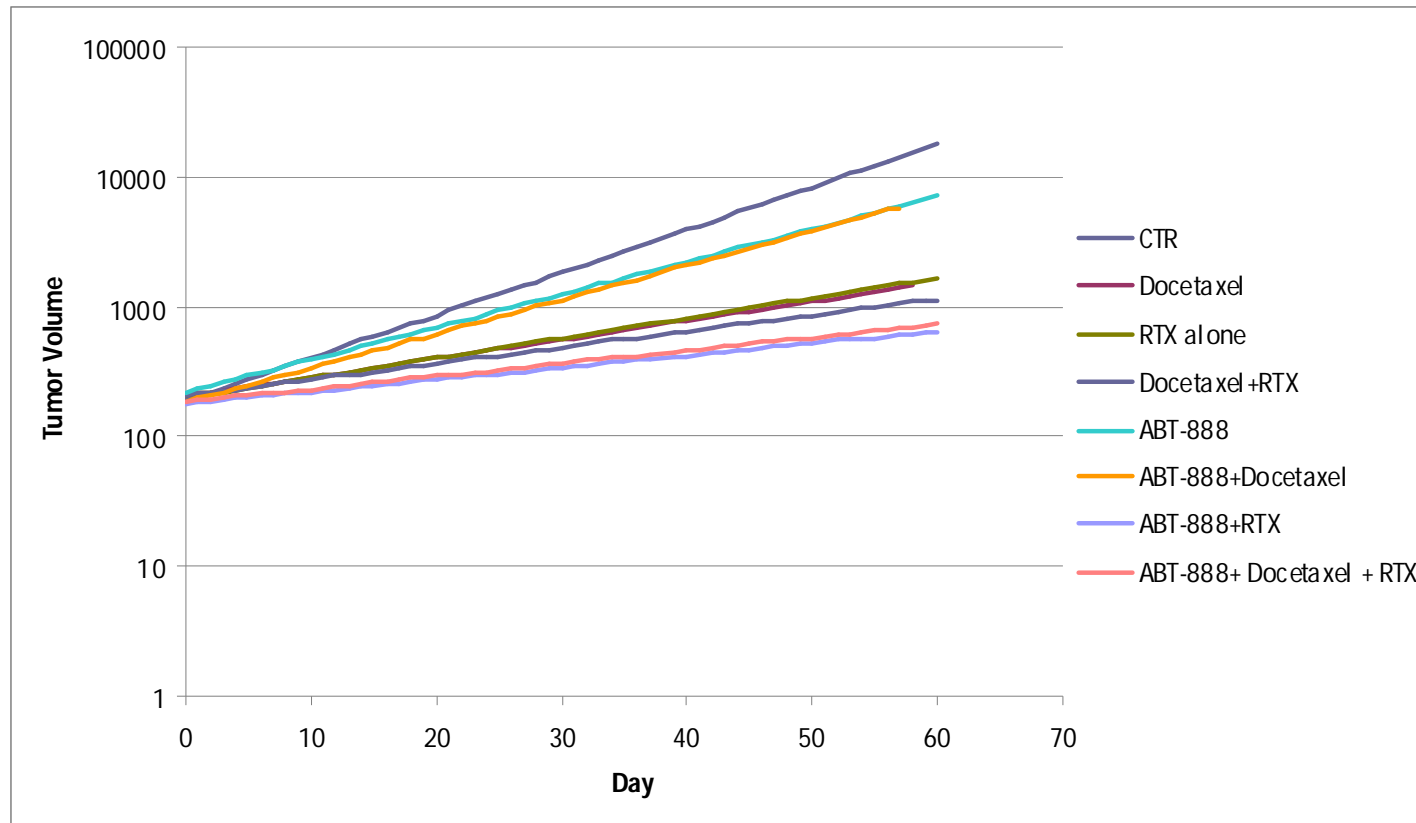


Figure 25. Model-estimated geometric mean tumor volume by group and time.

PC-3 xenografts

Table 7. Tumor growth rate (% change in volume per day) by group

Group	%Δ Volume (95% CI)	Tumor Doubling Time
Control	7.9 (5.9 , 9.8)	9.2 (7.4 , 12)
Docetaxel	3.4 (1.4 , 5.5)	20.6 (13 , 49.2)
RTX alone	3.6 (1.8 , 5.3)	19.8 (13.3 , 38.2)
Docetaxel+RTX	2.9 (0.9 , 4.9)	24.2 (14.4 , 77)
ABT-888	6 (4.2 , 7.8)	12 (9.3 , 17)
ABT-888+ Docetaxel	6.3 (3.9 , 8.7)	11.4 (8.3 , 18.2)
ABT-888 + RTX	2.2 (0 , 4.4)	32.3 (16.2 , 3460.1)
ABT-888+ Docetaxel + RTX	2.3 (0.4 , 4.2)	30.2 (16.7 , 158.4)

%Δ: estimated average rate of increase of tumor volume (% daily change) 100*(geometric mean ratio-1).

Table 8. Comparison of Growth Rates

Group Comparison	p-value for comparison of growth rates
RTX Alone vs. CTR	0.0017
ABT-888 vs. CTR	0.16
Docetaxel vs. CTR	0.0025
ABT-888+RTX vs. ABT-888	0.0096
ABT-888+RTX vs. RTX Alone	0.32
ABT-888+Docetaxel vs. ABT-888	0.83
ABT-888+Docetaxel vs. Docetaxel	0.075
Docetaxel+RTX vs Docetaxel	0.72
Docetaxel+RTX vs. RTX Alone	0.62
ABT-888+Docetaxel+RTX vs. ABT-888+ RTX	0.92
ABT-888+Docetaxel+RTX vs. ABT-888+ Docetaxel	0.012
ABT-888+Docetaxel+RTX vs. Docetaxel+RTX	0.68